Published in final edited form as:
J Am Chem Soc. 2009 November 25; 131(46): 16720–16734. doi:10.1021/ja9044357.

Pd-Catalyzed N-Arylation of Secondary Acyclic Amides: Catalyst Development, Scope, and Computational Study

Jacqueline D. Hicks, **Alan M. Hyde**[*,†], **Alberto Martinez Cuezva**[‡], and **Stephen L. Buchwald**[*]
Department of Chemistry, Massachusetts Institute of Technology, 77 Massachusetts Avenue, Cambridge, MA 02139

Abstract

We report the efficient N-arylation of acyclic secondary amides and related nucleophiles with aryl nonaflates, triflates, and chlorides. This method allows for easy variation of the aromatic component in tertiary aryl amides. A new biaryl phosphine with P-bound 3,5-(bis)trifluoromethylphenyl groups was found to be uniquely effective for this amidation. The critical aspects of the ligand were explored through synthetic, mechanistic, and computational studies. Systematic variation of the ligand revealed the importance of (1) a methoxy group on the aromatic carbon of the "top ring" *ortho* to the phosphorus and (2) two highly electron-withdrawing P-bound 3,5-(bis)trifluoromethylphenyl groups. Computational studies suggest the electron-deficient nature of the ligand is important in facilitating amide binding to the LPd(II)(Ph)(X) intermediate.

Introduction

Methods for the cross-coupling of amides with aryl halides and pseudohalides have matured to a point that they may be used to reliably prepare a wide variety of substances.[i] Advances in this area are due, in large part, to the identification of improved supporting ligands. The classic copper-mediated coupling of an amide with an aryl iodide (the Goldberg reaction) proceeds catalytically and at lower temperatures when diamine ligands are employed.[ii] Efficient Pd-catalyzed coupling of amides and related nucleophiles (ureas, carbamates, sulfonamides) with aryl bromides[iii] and aryl or vinyl sulfonates[iv] has largely been accomplished by the use of xantphos or XPhos as the supporting ligand. Most recently, the use of monodentate biarylphosphines bearing a methyl or methoxy group *ortho* to the phosphorus (**L3**) has enabled the coupling of amides with heteroaryl and aryl chlorides.[v,vi] A prominent limitation of all amidation methods is they are mostly restricted to primary amides or lactams—a general method for the intermolecular cross-coupling of acyclic secondary amides with aryl halides and/or pseudohalides has not yet been reported.[vii–ix] The large size of acyclic secondary amides,[3a] combined with their relatively low nucleophilicity (compared to amines), has made secondary amides a particularly challenging substrate class for cross-coupling.

Tertiary aryl amides and sulfonamides, the primary products described in this paper, are found in a variety of biologically active molecules (Figure 1).[x] Access to this class of compounds by arylation of the secondary amides would have advantages over traditional acylation strategies because it would allow for easy variation of the aromatic component, facilitating the generation

sbuchwal@mit.edu; ahyde@fas.harvard.edu.
[†]Corresponding Author for Theoretical Calculations.
[‡]Universidad de Burgos, Burgos, Spain.

Supporting Information Available: Experimental procedures and spectral data for all compounds, computational data, and kinetic plots. This material is available free of charge via the internet at http://pubs.acs.org.

of analogs for SAR studies. Additionally, secondary amides and carbamates are often intermediates in synthetic sequences[xi] and the ability to arylate these directly would improve the efficiency of synthetic routes.

Herein, we describe the rational development of a new biaryl phosphine (JackiePhos, **L6**) with P-bound 3,5-(bis)trifluoromethylphenyl groups, that facilitates amide binding by creating a more electrophilic Pd(II) intermediate. We have examined aspects of this catalyst system by synthetic, mechanistic, and computational investigations. The synthetic investigations will focus on: (1) substrate scope for the cross-coupling of secondary amides with aryl triflate and nonaflates, (2) cross-coupling of related nucleophiles (ureas, carbamates, sulfonamides), (3) extension of this method to include aryl chlorides, and (4) development of a diarylation process. The mechanistic investigations will focus on: (1) correlation of ligand structure to catalyst stability and (2) trends in aryl halide reactivity and the mechanistic implications. Finally, a computational study will examine each catalytic step for a series of related ligands in order to understand the effect of structural substitutions.

Results

In designing a new ligand for the N-arylation of secondary amides, we took into account existing knowledge of ligand effects and the mechanism of amidation. Xantphos, the standard ligand for the amidation of aryl iodides, bromides, and triflates, was ineffective as a ligand for the reaction in Chart 1. Instead we chose to focus our efforts on ligands derived from the BrettPhos biaryl motif[xii] (Chart 1), which contains two methoxy groups on the upper ring of the biaryl. This scaffold imparts properties that give catalysts superior performance in a number of C–N bond-forming transformations. Reactions employing BrettPhos[13] (**L2**) and *t*-Bu_2BrettPhos[5c] (**L3**) provided unsatisfactory yields of the desired product (27% and 21%, respectively). Based on our knowledge that "transmetallation" was rate-limiting for primary amides[5a] (and this step would likely be even more difficult for the larger secondary amides) we undertook the development of ligands that would facilitate this step. We hypothesized that a more electrophilic and less sterically-demanding Pd(II) intermediate was necessary to facilitate amide binding. Moreover, a similar strategy was employed by Beletskaya for the N-arylation of ureas in which an electron-deficient xantphos ligand possessing P-bound 3,5-(bis) trifluoromethylphenyl groups was shown to give the most active catalyst.[xiii] Toward this goal we prepared ligands **L4–L6**, in which the P-bound alkyl groups in **L2** and **L3** were replaced with aryl groups. The strongly electron-withdrawing 3,5-(bis)trifluoromethylphenyl substituent in ligand **L6** provided the most efficient ligand and the catalyst derived from **L6** provided the desired product in 87% yield. Consistent with our supposition, the conversion and product yields increased as the ligand became more electron-deficient (R = 3,5-CF_3Ph > 4-CF_3Ph > Ph).

Several other aspects of the reaction conditions utilized for the N-arylation of secondary amides deserve comment.[xiv] Aryl nonaflates (ArONf = $ArOSO_2(CF_2)_3CF_3$)[xv] were chosen as a cross-coupling partner because they are less susceptible to hydrolysis than aryl triflates, while still providing a similar, highly electrophilic, Pd(II) intermediate.[xvi,xvii] The use of a non-polar solvent such as toluene was found to be critical in obtaining high yields, whereas reactions in polar solvents (e.g., *t*-BuOH, DME) were less efficient. Additionally, the inclusion of molecular sieves in the reaction mixture improved the yields by inhibiting the formation of phenols and related side-products.[xviii] The $[(allyl)PdCl]_2$ precatalyst was chosen due to its ease of use and lack of coordinating ligands (such as dba).[xix] However, $Pd(OAc)_2$ could also be used if a preactivation step was employed in order to ensure formation of the Pd(0) complex.[5b]

Synthetic Investigations

With optimized reaction conditions in hand, we examined the scope of the method. Secondary amides coupled efficiently with a variety of electron-deficient, electron-neutral, and moderately electron-rich aryl nonaflates—with electron-deficient aryl nonaflates typically giving the highest yields (Table 1, entries 1–3). α-Branched amides reacted smoothly (entries 5 and 6), but branched alkyl substitution on the nitrogen was not tolerated. In addition to nonaflates, aryl triflates were also successfully converted to product (entries 7 and 8). In difunctionalized substrates, it was found (unsurprisingly) that the nonaflate group reacted in preference to a chloride substituent (entries 9 and 10). A relatively small group at the *ortho* position of the aryl sulfonate such as Cl was tolerated, but larger substituents were not. Acetanilide and other *N*-aryl amides are traditionally difficult substrates for Pd-catalyzed cross-coupling reactions, but by using a slight modification of our general protocol, employing K_3PO_4 as the base, acetanilide could be N-arylated in 78% yield (entry 11).[xx] We note that attempts to realize the same product from the aryl bromide using xantphos as the supporting ligand gave a very low yield of the product.[xxi]

Given the successful coupling of secondary amides, we next examined the reaction of carbamates, ureas, and sulfonamides. Substituted ureas proved to be difficult substrates and could only be coupled with electron-deficient nonaflates, and then only in moderate yields (Table 2, entries 1 and 2). In contrast, secondary carbamates, which are less sterically demanding, were excellent substrates. The coupling of Boc- and Cbz-protected amines proceeded in 87% and 90% yield, respectively (entries 3 and 6). The use of secondary sulfonamides also provided good yields of coupled products (entries 7–9). These examples are significant because there are only isolated examples of the successful cross-coupling of *N*-alkyl carbamates[xxii] and to the best of our knowledge, the intermolecular coupling of *N*-alkyl acyclic sulfonamides or *N*-alkyl, *N*′,*N*′-dialkyl ureas has not yet been reported.

In order to expand the utility of this method, we sought to develop conditions that would allow for the coupling of secondary amides with aryl chlorides. Many aryl chlorides are commercially available and the ability to utilize these substrates would improve the generality of this method.[xxiii] Increasing the reaction temperature and utilizing Cs_2CO_3 as the base provided good yields of amidation products. The substrate scope of the aryl chloride coupling was briefly examined as shown in Table 3. A variety of aryl chlorides were successfully coupled with secondary amides as well as with a secondary carbamate (entry 4) and a secondary sulfonamide (entry 5). The reaction of more hindered amides proved to be difficult with aryl chlorides; for those substrates in particular, aryl triflates/nonaflates are recommended as the coupling partners.

Given our success in coupling *N*-aryl amides with aryl nonaflates and chlorides, we examined the diarylation of a primary amide.[xxiv] By combining a primary amide with 2.2 equivalents of aryl halide or pseudohalide and three equivalents of base under otherwise identical reaction conditions to that described above, good yields of the desired *N*,*N*-diaryl amides could be obtained (Table 4). This diarylation method allows for the rapid synthesis of diaryl benzamide derivatives. These compounds exhibit interesting biological activity as nuclear receptor binding agents.[xxv] An example is 3-hydroxy-*N*,*N*-diphenylbenzamide, which alters pS2/TFF1 expression levels. (pS2/TFF1 is important in maintaining gastric mucosal integrity and may act as a tumor suppressor signal in the stomach.[xxvi]) Through the diarylation of 3-methoxybenzamide (entries 4–6), a series of 3-hydroxy-*N*,*N*-diphenylbenzamide analogs were readily available.

Mechanistic Investigation

Our recent studies on C–N bond formation have shown that ligands containing methoxy groups on the upper ring of the biaryl backbone provide significantly better results than those without the substituent. In order to probe the importance of the methoxy groups, a series of JackiePhos analogs were prepared and tested. Ligands **L7–L9** (Table 5), containing variable substitution on the upper biaryl ring, were examined under standard reaction conditions for the coupling of *N*-butylacetamide and of 4-*t*-butylphenyl nonaflate. The catalyst derived from ligand **L9**, containing only one methoxy substituent *ortho* to the phosphorus led to successful amidation. Yields for amidation reactions using **L9** were similar to those obtained with JackiePhos, and monitoring the amidation with *in situ* IR indicated that the reaction profiles were nearly identical. However, the catalyst derived from ligand **L7**, lacking both of the methoxy groups, provided only 5% of the desired product and quickly degraded to palladium black. This indicates that the upper methoxy *ortho* to the phosphorus is of critical importance to catalyst stability. To determine if this was simply a steric effect, ligand **L8** containing an *ortho* methyl group was synthesized. Interestingly, **L8** was not a useful ligand for amidation reactions despite NMR experiments showing it undergoes oxidative addition to PhCl. Thus, the methoxy group *ortho* to the phosphorus of JackiePhos cannot be substituted with a slightly larger, non-coordinating group.

To better understand the relative reactivity of the aryl halide or pseudohalide in these amidation reactions, we compared the reaction profiles of phenyl triflate, iodobenzene, bromobenzene, and chlorobenzene with *N*-butyl acetamide. The reactions were monitored for product formation by *in situ* IR spectroscopy (Chart 2). The reaction of *N*-butyl acetamide with phenyl triflate proceeded to completion in just over 5 hours. In contrast, the reaction of aryl halides did not reach completion in 22 hours. We observed some unexpected trends in the reactions of the aryl halides—the reaction of chlorobenzene was significantly faster than that of bromobenzene, which in turn was much faster than iodobenzene, which produced essentially no product. The general trend of ArOTf/ArONf > ArCl > ArBr > ArI was also observed for the other substituted aryl halides/pseudohalides examined.

To gain a more thorough understanding of the origin of these trends, we carried out several competition experiments. In Table 6 a comparison of the yields for the cross-coupling of *N*-butyl acetamide with aryl electrophiles under the optimal reaction conditions developed for aryl chlorides is shown. The yields given in this table are consistent with the relative reactivity of this series of substrates. Given that aryl chlorides react faster under these conditions than the corresponding aryl bromides, we performed a competition experiment between 1-*n*-butyl-4-chlorobenzene and 4-bromotoluene (eq 1). As expected, exclusive cross-coupling with the 4-bromotoluene was observed, consistent with a mechanism in which oxidative addition occurs preferentially with 4-bromotoluene. A similar competition experiment between 1-*n*-butyl-4-chlorobenzene and 4-iodotoluene provided no cross-coupled product (eq 2), demonstrating that oxidative addition occurred with 4-iodotoluene in preference to 1-*n*-butyl-4-chlorobenzene. These results strongly disfavor a mechanism in which oxidative addition affects the observed rate, but instead are consistent with the idea that "transmetallation" step is responsible for the observed trend in reactivity. In our previous kinetic studies on amidation, the faster rate of "transmetallation" for aryl triflates was attributed to a more labile LPd(Ph)OTf complex compared to LPd(Ph)halide complexes.[5a] Analogously, the rate of amide/amidate attack on LPd(Ph)Cl may be faster than attack on LPd(Ph)Br due to the more electrophilic nature of palladium in LPd(Ph)Cl. This is supported by the trend in rates of associative ligand exchange of $[Pt(dien)X]^{n+}$ complexes, following the order Cl > Br > I.[xxvii]

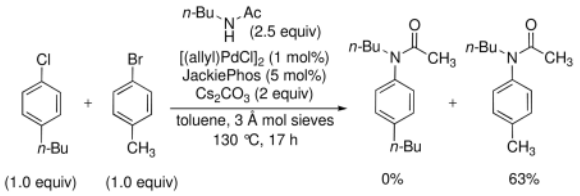

(1)

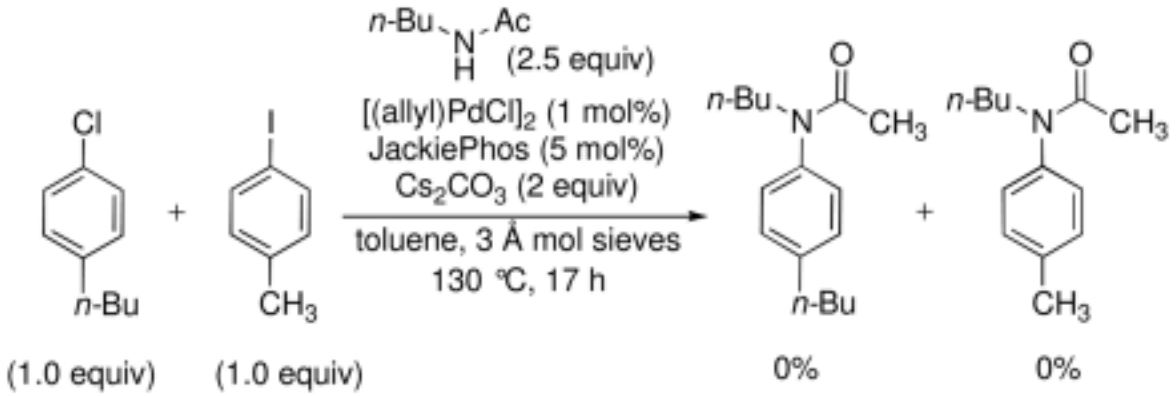

(2)

Computational Studies

Future advances in the design of biarylmonophosphine ligands would benefit from a firm understanding of the effects bestowed by substituents appended to the biaryl backbone. Although we were pleased with the superior performance of JackiePhos in comparison to other biarylmonophosphine ligands, we sought further mechanistic support for our original hypothesis that its electron withdrawing nature allows for faster transmetallation; this prompted us to investigate the role of the structural features present in this ligand. For these studies, we chose to focus on two points: (1) determination of the effect of substitution of different P-bound R groups (i.e., 3,5-CF_3Ph, *t*-Bu, Cy, Ph) and (2) the development of an understanding of the role of the methoxy group bound to the upper ring *ortho* to the phosphorus.

Since we were unable to measure the relative rates of each mechanistic step due to difficulties in isolating catalytic intermediates, we turned instead to a computational approach using DFT methods. Computational investigations of Pd-catalyzed cross-coupling reactions have become increasingly routine, but an examination of the literature reveals that the majority of these analyses are limited to catalysts containing small phosphines (e.g., PH_3, PMe_3, $H_2PCH_2CH_2PH_2$) that serve as models for larger ligands (e.g., PPh_3, P(*t*-Bu)$_3$, $Ph_2PCH_2CH_2PPh_2$).[xxviii] While the conclusions from these studies have provided much insight into the operative mechanism of these processes, many difficult cross-coupling reactions do not proceed with these simple ligands. Therefore, caution should be exercised when applying approximations to ligands when examining such reactions.[xxix]

With the rapid increases in computational power and concurrent decrease in cost, we favor a more rigorous approach, which entails modeling the complete catalyst with all-atom DFT. We believe that studying the subtle structural features of the ligand is critical for a thorough

mechanistic understanding. Furthermore, in the following discussion we compare several related biaryl monophosphines that behave markedly different in promoting catalysis. The direct comparison of ancillary phosphine ligands by computational methods represents an infrequently used but powerful approach to understanding intricate details of critical mechanistic processes.[28a,xxx]

Our strategy to unraveling the structure/activity relationship of these ligands was to systematically change one portion of the ligand and calculate the effect on each step of the catalytic cycle. Scheme 1 shows the general outline of the possible steps in the catalytic cycle we would examine—oxidative addition (eq 1), associative ligand exchange (eq 2), dissociative ligand exchange (eq 3), formation of the κ^2-bound amidate (eq 4), and reductive elimination (eq 5). The ligands we opted to focus on were **L1** (xantphos), **L6** (JackiePhos), **L2** (BrettPhos), **L3** (*t*-Bu_2BrettPhos), **L4** (Ph_2BrettPhos), and **L10** (a simplified version of **L8**), which are shown in Scheme 1. Xantphos was included in this comparison since it is a very effective ligand for many amidation reactions[3a–h, 4a,b] and its role in Pd-catalyzed cross-couplings has never been studied computationally.[xxxi] It also serves as a benchmark for comparison to our biarylmonophosphine ligands, and to validate our computational results by further correlation with experiment. Our justification for modeling **L10** instead of **L8** rests on previous studies that demonstrate only the methyl group *ortho* to the phosphorus influences the properties of these ligands in amidation reactions.[5a]

Methods

All calculations were performed using the Gaussian ’03 suite of programs,[xxxii] primarily with Dell PowerEdge 1950 servers containing two quad-core Intel Xeon processors or Sun servers containing dual-core Opteron processors, running the sun grid engine (SGE) queuing program. We also made use of supercomputing resources for potential energy scans. Ground-state geometry optimizations were performed with the Berny algorithm using all-atom DFT (B3LYP/6-31(d)) and the LANL2DZ basis set with the Hay–Wadt[xxxiii] effective core potential (ECP) for all Pd and Br atoms. Frequency calculations were performed on all optimized structures to confirm that the minima had no negative frequencies and transition states had a single imaginary frequency. The Gibbs free energies were calculated at 298.15 K and 1 atm. Single point calculations were then performed with the 6-311+g(2d,p) basis set to obtain higher accuracy electronic energies. Solvation effects were calculated at the 6-311+g(2d,p) level with the CPCM method[xxxiv] in conjunction with the UAKS cavity and employing a dielectric constant of $\varepsilon = 2.374$ for toluene. Basis set superposition error (BSSE) was corrected for by use of the counterpoise method of Boys and Bernardi.[xxxv] Although BSSE is a general phenomenon when using incomplete basis sets, correcting for it is critical when constructing potential energy diagrams.[xxxvi]

Oxidative Addition

As stated earlier, it is unlikely that oxidative addition is the rate-limiting step in most Pd-catalyzed amide arylation reactions based on previous work performed in our group.[5a] Nevertheless, the barriers for this step were calculated (Table 7), as the rate-limiting step could change for some ligands. We began by finding the barrier of oxidative addition to bromobenzene (**1-TS**, entry 1) and chlorobenzene (**2-TS**, entry 2) with xantphos·Pd (**1**). Interestingly, the geometry of these transitions states were pseudotetrahedral about the Pd center as opposed to the more common square planar conformation, probably a result of the large bite angle of xantphos.[xxxvii] Alternative transition states with *cis* or O-bound geometries could not be located. A moderate barrier of 26.8 kcal/mol was calculated for **1-TS**, but a high barrier of 36.6 kcal/mol was calculated for **2-TS**. This is consistent with the experimental observation that the use of xantphos does not allow for the Pd-catalyzed cross-coupling of unactivated aryl chlorides.[5a,xxxviii]

We found four energy minimized oxidative addition complexes for xantphos·Pd(Ph)(Br), shown in Table 8. The tetrahedral transition state **1-TS** initially leads to the highest energy tetrahedral isomer **2a** (confirmed by an IRC calculation), which then can isomerize to the lower energy *trans*[xxxix] (**2b**), O-bound (**2c**) or *cis* (**2d**) complexes. The bond angles and bond lengths about the Pd center are listed and illustrate the large range of conformations the xantphos catalyst can adopt, underscoring the dynamic nature of this ligand. The O5–Pd–P3 bond angle of **2c** is only 76.0° while the P1–Pd–P2 bond angle ranges from 104.9° in **2d** to 113.3° in **2a** to 146.2° in **2b**.

Although aryl chlorides, triflates, and nonaflates are all capable coupling partners when using JackiePhos, we chose to focus on modeling oxidative addition with chlorobenzene as it would simplify the calculations and corresponds to the most difficult case in the series that we studied. In Table 9, the calculated barriers for oxidative addition to chlorobenzene with Pd(0) complexes of JackiePhos (entry 1), BrettPhos (entry 2), *t*-Bu_2BrettPhos (entry 3), Ph_2BrettPhos (entry 4), and **L10** (entry 5) are listed. They are quite low—even for electron-deficient ligands—ranging between 10.8 and 20.4 kcal/mol, and are in agreement with our previous computational study[29b] on the reactivity of SPhos·Pd and XPhos·Pd. The low barrier calculated for JackiePhos (20.1 kcal/mol, entry 1) supports our assertion that this step is not rate-limiting. It is interesting that even though JackiePhos is significantly more electron-deficient than xantphos, the barrier to oxidative addition of chlorobenzene with the former is over 16 kcal/mol lower in energy. This is consistent with previous findings from our laboratory concerning the relative importance of steric and electronic factors on the rates of cross-coupling reactions.[xl]

Associative Transmetallation

The step following oxidative addition is “transmetallation”, in which ligand exchange of an amide for a halide probably occurs either by an associative or dissociative mechanism. Given the pK_a difference between amides (15.1 for N–H) and carbonate (10.3), we believe that deprotonation occurs following amide binding to the Lewis acidic Pd(II) center. If an associative mechanism is operative, then the amide must first bind to Pd, giving rise to a five-coordinate intermediate in the case of xantphos and a four-coordinate intermediate in the case of monophosphines, followed by deprotonation and halide dissociation. An examination of the literature reveals very few mechanistic details concerning ligand substitution with amides either experimentally or theoretically.

The amide included in our calculations was *N*-methyl acetamide, which was chosen to be representative of secondary, acyclic, alkyl amides. The calculated geometry of the four-coordinate *trans*-xantphos·Pd(Ph)(Br) complex **2b**, and five-coordinate square pyramidal complex **8** with an O-bound amide are shown in Scheme 2. This binding is endothermic by 28.7 kcal/mol of energy and results in a fairly weak Pd–Br interaction in the axial position with a bond length of 3.22 Å. A similar structure with a triflate counterion could not be located.

The binding energies of *N*-methyl acetamide to each biaryl monophosphine·Pd(Ph)(Cl) complex were next determined (Table 10). We first calculated the energy of amide binding to the JackiePhos·Pd(Ph)(Cl) complex in cases where the Pd center is pointed away from the lower biaryl ring (complexes **9b–d**). The most favorable interaction, being endothermic by 18.2 kcal/mol,[xli] occurred when the amide was bound to Pd through its oxygen atom and oriented *cis* to the phosphorous (**9b**). The energy of amide binding with the Pd but centered over the bottom ring was also calculated and was significantly higher in energy in both possible configurations (**9f**, 26.4 kcal/mol and **9g**, 25.1 kcal/mol). The energies of the other L·Pd(Ph)(Cl)(amide) adducts in configuration **b** were next calculated. We also verified that the lowest energy configuration for JackiePhos held for other ligands and they did with the exception of isomer **f**. For BrettPhos and *t*-Bu_2BrettPhos, this isomer was not a stationary state but we found that isomer **g** oriented with the amide *trans* to the phosphorus did represent a stable minimum.

Larger energies for amide binding were calculated for BrettPhos-(23.0 kcal/mol, **10b**) and *t*-Bu_2BrettPhos-(23.5 kcal/mol, **11b**) ligated complexes. In contrast, with Ph_2BrettPhos, a significantly lower energy for this step (19.8 kcal/mol, **12b**) was calculated. As in the oxidative addition step, **L10** is calculated to behave similarly to JackiePhos; its oxidative addition complex requires only 17.5 kcal/mol for amide binding.

Further information on the mechanism of this step would be gained from examining transition states for amide attack and amide deprotonation. However, our efforts to locate such structures were unsuccessful and at this point we can only qualitatively say that they will be higher in energy than the corresponding ground states.

The accessibility of isomer **b** in Table 10 relies on the free rotation about the C_{aryl}–P bond, which has been shown in previous computational studies to be quite difficult for Me_4*t*-Bu_2XPhos·Pd(Ph)(amidate).[5a] The JackiePhos·Pd(Ph)(amidate) complex is likely to have a lower barrier of rotation for two reasons: first, the methoxy group *ortho* to phosphorous is smaller than the methyl group in Me_4*t*-Bu_2XPhos, and second, the P-bound arenes of JackiePhos are much smaller than the bulky *t*-Bu groups of Me_4*t*-Bu_2XPhos. In order to support this assertion, we performed a potential energy scan about the C_{aryl}–P bond in which a restricted structure optimization was executed at every 10°. We chose to calculate this with the JackiePhos·Pd(Ph)(amidate) complex because it, too, would need to freely rotate once formed and, being larger than the chloride complex, would be the more difficult case. The maxima of the resulting energy curve, shown in Figure 2, corresponds to a barrier of rotation of 19.8 kcal/mol—an amount of energy that is readily overcome even at room temperature.

We next performed potential energy scans about the C2–P3 bond with analogous complexes containing the other ligands and very similar curves were obtained (not shown). However, the maximum for the BrettPhos complex lies at a dihedral angle of 90° while all of the other ligands gave maxima at 80°. The barrier heights for these complexes are listed in Table 11: JackiePhos (entry 1), BrettPhos (entry 2), and Ph_2BrettPhos (entry 4) give barriers of very similar energies (19.2, 20.5, and 19.1 kcal/mol, respectively). Of note is that switching the methoxy group of the upper ring to a methyl group in JackiePhos increases the barrier significantly to 23.3 kcal/mol (entry 5), presumably because of its larger size. We also found that the barrier to rotation for the most sterically congested ligand, *t*-Bu_2BrettPhos (entry 3), is only 27.7 kcal/mol (compared to 33 kcal/mol for Me_4*t*-Bu_2XPhos[5a]). It follows from the Eyring equation that this barrier corresponds to a half life of only 9.16 min at 110 °C assuming a first order rate law. Based on these data, we conclude that under the reaction conditions (110–130 °C) all the ligands including *t*-Bu_2BrettPhos can freely rotate with the Pd moiety being either over or away from the lower biaryl ring.

Dissociative Transmetallation

The loss of a halide/pseudohalide to form cationic Pd(II) intermediates is quite common in Heck-type processes,[xlii] but is not necessary for most cross-coupling reactions in which an organometallic component participates as the nucleophile. However, this pathway should be considered for reactions involving weakly-nucleophilic, non-metallic partners, such as hindered amides. Furthermore, dissociative ligand exchange through a cationic Pd(II) intermediate has been suggested by van Leeuwen to occur for xantphos-Pd(II) complexes undergoing *cis*/*trans* isomerization[39a] and in the amination of aryl triflates[xliii].

For the following calculations, we deemed it important to model both the bromide and triflate, as the latter are so much more effective as leaving groups.[xliv] It was critical for the inclusion of solvation effects for this step as dissociation was highly endothermic in the gas phase. As depicted in Table 12, the energy difference between cationic complex **14** and both the *trans*-xantphos·Pd(Ph)(Br) (**2b**) and *trans*-xantphos·Pd(Ph)(OTf) (**15**) complexes were determined.

The loss of the bromide is endothermic by 17.5 kcal/mol but loss of triflate is endothermic by only 0.8 kcal/mol. It should be pointed out that correction for BSSE was critical for Br dissociation as it was originally in error by 16.5 kcal/mol, while triflate dissociation was only in error by 3.2 kcal/mol (a more typical value). The unusually large error in the first case is likely a result of the use of the approximations implicit in the LANL2DZ basis set for an entire fragment.[xlv]

The ionization energy requirement for the bromide complex could be low enough to outcompete the associative pathway. For aryl triflates, the nearly equal energies of **14** and **15**, our inability to locate a 5-coordinate amide-bound Pd-triflate complex as well as structural characterization by van Leeuwen[39a] of a cationic xantphos·Pd(Ar)(OTf) complex are good evidence that ligand exchange occurs by a dissociative pathway. However, based on the experimental results that more hindered amides (e.g., those that are the focus of this paper) are not readily arylated with a xantphos/Pd catalyst and reductive elimination should not be difficult (*vide infra*), we must conclude that there is also a significant energy cost to approach of the amide and/or isomerization from O- to N-bound isomers.

With a handle on the difference in energy for ionization in xantphos·Pd(Ph)(OTf/Br) complexes, we were prompted to perform similar calculations on the JackiePhos·Pd(Ph)(OTf/Cl) complexes (Table 13). The empty coordination site in the cationic product may be *cis* or *trans* to the phosphorous, but structures in which the empty site is *trans* to the phosphorous were much lower in energy and are the only ones considered here. Additionally, the Pd may be pointed away from the bottom ring, in which it has a dative bond with the oxygen, or towards the lower ring, in which it interacts with the π-electrons of the arene. Surprisingly, C-bound isomer **18** is significantly lower in energy than O-bound isomer **17**. Unlike the xantphos system, however, ionization of both the chloride (42.9 kcal/mol to reach **18**) and triflate (34.9 kcal/mol to reach **18**) were prohibitively high in energy. The resistance to ionization of the JackiePhos system is probably a consequence of the Pd being both coordinatively unsaturated and electron poor.

κ^2-Binding of the Amide to Pd

Previous work has demonstrated that Pd-catalyzed amidation reactions are complicated by the formation of κ^2-amidate complexes in which the amide is simultaneously bound to the palladium center at both the nitrogen and oxygen atoms.[39b] In these studies, it was shown that κ^2-amidate complexes do not undergo reductive elimination as readily as κ^1-amidate complexes. While some monophosphine ligands may not be effective ligands for amidation as they allow κ^2-amidate formation, we have previously shown that bulky monodentate biaryl phosphines can form effective catalysts for amidation.[4c,5] In light of the experimental evidence presented,[39b] suggesting that catalyst inhibition and inactivation results from κ^2-binding, we calculated the relative energies of κ^1- and κ^2-bound isomers of both xantphos·Pd(Ph)(amidate) and JackiePhos·Pd(Ph)(amidate) complexes. Quite unexpectedly, the κ^2-bound xantphos structure (**20**) is calculated to be lower in energy than the *cis*-κ^1-bound structure (**19**) by 9.3 kcal/mol (Scheme 3). This energy is seemingly in disagreement with the previously reported IR and NMR data obtained for xantphos·(Ph)(*N*-phenylacetamide) complexes that support κ^1-bound structures as being more stable.[39b] However, the amide-bound complexes in this study were prepared by the addition of potassium amides to xantphos·Pd(Ph)(Br) at room temperature, and the thermodynamically more stable isomer may have not been kinetically accessible. Similarly, JackiePhos·Pd(Ph)(amidate) favors κ^2-bound structures, pointed both towards (**22**, −2.3 kcal/mol) and away (**23**, −3.7 kcal/mol) from the lower biaryl ring (Scheme 4). In contrast to the xantphos system, the barrier to reach these structures is probably not as high since there is an open coordination site on Pd. Based on these results, we believe κ^2-binding does not necessarily lead to decomposition or inhibit catalysis (i.e., it can form

reversibly), but rather, it may lie on the path to catalyst decomposition for unhindered monodentate ligands.

Reductive Elimination

Reductive elimination is often the most difficult step for the arylation of weaker nucleophiles such as amides.[xlvi] We first calculated the barrier for C–N bond formation from the xantphos·Pd(Ph)(amidate) complex and found it was 20.4 kcal/mol (**8-TS**, Scheme 5). In contrast to the tetrahedral geometry in the transition state for oxidative addition, this geometry is square planar, proceeding from *cis*-complex **19**. We believe that a tetrahedral transition state similar in geometry to those found for oxidative addition (Table 7) is no longer accessible due to the larger size of the amide compared to bromide.

Next, we compared the barrier to C–N bond formation for each of the biaryl monophosphine ligands (Table 14).[xlvii] The ligands that allowed for the lowest barriers of reductive elimination (16.6 kcal/mol for both) were *t*-Bu_2BrettPhos (**11-TS**, entry 2) and **L10** (**13-TS**, entry 5), while the barrier for this step was slightly higher with JackiePhos (17.7 kcal/mol, entry 1). Both BrettPhos and Ph_2BrettPhos were predicted to be less effective at promoting this step, with barriers of 19.7 (entry 2) and 20.0 kcal/mol (entry 4), respectively.

Five-membered cyclic transition states were also found in which an O-bound amidate pivots back towards the reactive Ph group to form a C–N bond (Figure 3). In both the case of xantphos (**14-TS**, 23.0 kcal/mol) and JackiePhos (**15-TS**, 22.0 kcal/mol), this transition state was higher in energy, leading us to believe that it constitutes a minor pathway for this reaction. However, it may be more important in the arylation of other less hindered amides or if O to N isomerization proves difficult.

Catalytic Cycle

Without an analysis of a continuous potential energy diagram for the catalytic cycle, the relative contributions from each mechanistic step are not entirely clear. Accordingly, the relative energies of each step through the amide binding event were connected in Figures 4 and 5 so that such an analysis could be performed. We did not construct a potential energy diagram for the entire catalytic cycle because of the uncertainties in the barriers to transmetallation as well as the energy change for salt precipitation and dissolution, as this is a heterogeneous reaction.

First, in Figure 4, the potential energy diagram for the xantphos-Pd catalyst is depicted. Although aryl triflates likely react through a dissociative pathway, we will examine the energy pathway for the aryl bromide case because it will be more comparable to the mechanism involving the biarylmonophosphine-derived catalysts. In the catalytic cycle with bromobenzene, oxidative addition is slightly endothermic by +3.3 kcal/mol based on the difference between **1** with bromobenzene and the most stable *trans*-xantphos-Pd(II) isomer (**2b**). Assuming transmetallation operates by associative ligand exchange, amide binding (**8**) brings the total energy needed to 32.0 kcal/mol.

The information contained in the potential energy diagram of the biarylmonophosphine-Pd catalysts in Figure 5 is not as readily apparent as in Figure 4. First, the thermodynamics of oxidative addition to reach **C** is drastically different for each catalyst, all being exothermic but with an energy change ranging between −0.2 and −13.8 kcal/mol. As a consequence, the more exothermic this step becomes, the more energy that will be required to scale the subsequent reaction barriers. In this scenario, the energy requirement for catalysis will not be the energy change from starting materials to the highest barrier but the difference between the lowest point (**C**) and the highest barrier. In the cases of *t*-Bu_2BrettPhos and **L10**, the energy for bond rotation

(**D**) is the highest peak in Figure 5, but we believe that with consideration of the barriers for transmetallation and reductive elimination it will not be rate-limiting.

Although we lack the information to give predicted energy requirements and overall rates for each catalyst, we find that the energy differences from the lowest energy point and the amide-bound complex correlate well with ligand performance in most cases. These energies are listed in Table 15 and the smallest energy requirement is associated with JackiePhos (18.2 kcal/mol) and **L10** (17.5 kcal/mol). We feel that the trends shown here will be consistent but amplified when considering the barriers for amide attack and deprotonation. Since **L10** is calculated to perform equally well or better than JackiePhos in each mechanistic step but is completely ineffective in promoting the reaction, we believe the catalyst formed from it is not stable under the reaction conditions, degrading by an as yet undetermined pathway.

Conclusions

In summary, we have reported an efficient method for the N-arylation of acyclic secondary amides with aryl nonaflates, triflates, and chlorides. The catalyst system is also useful for the N-arylation secondary carbamates, ureas, and sulfonamides and the diarylation of primary amides. A ligand for this transformation, JackiePhos (**L6**), was designed based on the knowledge that "transmetallation" was rate-limiting for the arylation of primary amides and the hypothesis that a more electrophilic and less sterically demanding Pd(II) intermediate would facilitate the "transmetallation" of secondary amides. Our synthetic, mechanistic, and computational studies showed the success of JackiePhos is due to: (1) the methoxy group *ortho* to the phosphorus and (2) the strongly electron-withdrawing P-bound 3,5-(bis) trifluoromethylphenyl groups.

Theoretical studies have provided insight into the mechanism of "transmetallation" and show that the lowest energy conformation for amide binding occurs while Pd is pointed away from the lower biaryl ring. A potential energy scan about the C_{aryl}–P bond indicates that this conformation, in which Pd interacts with the methoxy group *ortho* to the phosphorus, is quite accessible. Our synthetic studies show that the *ortho* methoxy group is critical for catalyst stability and cannot removed or substituted with a methyl group. Additionally, computational studies predict the most favorable energies of amide binding for ligands containing the highly electron-withdrawing P-bound 3,5-(bis)trifluoromethylphenyl groups. Overall, it seems the "transmetallation" of secondary amides is facilitated by the ability of the ligand to access a highly electrophilic Pd(II) intermediate where the Pd is oriented away from the bottom ring of the biaryl backbone and stabilized by the *ortho* methoxy group. Additionally, the barrier to reductive elimination was lower for the electron-deficient JackiePhos compared to other sterically similar ligands (Ph_2BrettPhos, **L4**). However, there remain many questions on the precise mechanism and energetic requirements of the transmetallation step, preventing the construction of a full potential energy diagram. Overall, these studies further expand our understanding of structural features of biarylmonophosphine ligands and how each of these contributes to the catalysts derived from them.

Supplementary Material

Refer to Web version on PubMed Central for supplementary material.

Acknowledgments

We thank the National Institutes of Health (NIH) for funding this project (Grant GM-58160). We thank Merck, Boehringer Ingelheim, BASF (Pd compounds), Chemetall (Cs_2CO_3) and Nippon Chemical for additional support and the National Science Foundation through the National Center for Supercomputing Applications (NCSA), which

provided supercomputing resources. We are grateful to B. P. Fors for carrying out additional experiments to address reviewer comments.

References

i. For reviews, see: (a) Ley SV, Thomas AW. Angew Chem, Int Ed 2003;42:5400. (b) Kunz K, Scholz U, Ganzer D. Synlett 2003:2428. (c) Ma D, Cai Q. Acc Chem Res 2008;41:1450. [PubMed: 18698852] (d) Jiang, L.; Buchwald, SL. Metal-Catalyzed Cross-Coupling Reactions. Vol. 2. de Meijere, A.; Diederich, F., editors. Wiley-VCH; Weinheim, Germany: 2004. (e) Surry DS, Buchwald SL. Angew Chem, Int Ed 2008;47:6338.

ii. For Cu-catalyzed reactions, see: (a) Shen R, Porco JA. Org Lett 2000;2:1333. [PubMed: 10810741] (b) Klapars A, Antilla JC, Huang X, Buchwald SL. J Am Chem Soc 2001;123:7727. [PubMed: 11481007] (c) Klapars A, Huang X, Buchwald SL. J Am Chem Soc 2002;124:7421. [PubMed: 12071751] (d) Jiang L, Job GE, Klapars A, Buchwald SL. Org Lett 2003;5:3667. [PubMed: 14507200] (e) Klapars A, Parris S, Anderson KW, Buchwald SL. J Am Chem Soc 2004;126:3529. [PubMed: 15025480] (f) Pan X, Cai Q, Ma D. Org Lett 2004;6:1809. [PubMed: 15151420] (g) Strieter ER, Blackmond DG, Buchwald SL. J Am Chem Soc 2005;127:4120. [PubMed: 15783164] (h) Strieter ER, Bhayana B, Buchwald SL. J Am Chem Soc 2009;131:78. [PubMed: 19072233]

iii. For the use of xantphos, see: (a) Yin J, Buchwald SL. Org Lett 2000;2:1101. [PubMed: 10804564] (b) Yin J, Buchwald SL. J Am Chem Soc 2002;124:6043. [PubMed: 12022838] (c) Shen Q, Hartwig JF. J Am Chem Soc 2007;129:7734. [PubMed: 17542591] (d) Huang J, Chen Y, King AO, Dilmeghani M, Larsen RD, Faul MM. Org Lett 2008;10:2609. [PubMed: 18491862] (e) Manley PJ, Bilodeau MT. Org Lett 2004;6:2433. [PubMed: 15228297] (f) Audisio D, Messaoudi S, Peyrat JF, Brion JD, Alami M. Tetrahedron Lett 2007;48:6928. (g) Messaoudi S, Audisio D, Brion JD, Alami M. Tetrahedron 2007;63:10202. (h) Artamkina GA, Sergeev AG, Beletskaya IP. Tetrahedron Lett 2001;42:4381.For the use of $P(t\text{-}Bu)_3$, see: (i) Hartwig JF, Kawatsura M, Hauck SI, Shaughnessy KH, Alcazar-Roman LM. J Org Chem 1999;64:5575. [PubMed: 11674624]

iv. For the use of xantphos, see: Refs 3a,b (a) Wallace DJ, Klauber DJ, Chen C, Volante RP. Org Lett 2003;5:4749. [PubMed: 14627431] (b) Imbriglio JE, DiRocco D, Raghavan S, Ball RG, Tsou N, Mosley RT, Tata TR, Collitti SL. Tetrahedron Lett 2008;49:4897.For the use of XPhos, see: (c) Huang X, Anderson KW, Zim D, Jiang L, Klapars A, Buchwald SL. J Am Chem Soc 2003;125:6653. [PubMed: 12769573] (d) Bhagwanth S, Waterson AG, Adjabeng GM, Hornberger KR. J Org Chem 2009;74:4634. [PubMed: 19518153] For the use of other ligands, see: (e) Klapars A, Campos KR, Chen C, Volant RP. Org Lett 2005;7:1185. [PubMed: 15760170] (f) Willis MC, Brace GN, Holmes IP. Synthesis 2005:3229.

5. (a) Ikawa T, Barder TE, Biscoe MR, Buchwald SL. J Am Chem Soc 2007;129:13001. [PubMed: 17918833] (b) Fors BP, Krattiger P, Strieter E, Buchwald SL. Org Lett 2008;10:3505. [PubMed: 18620415] (c) Fors BP, Dooleweerdt K, Zeng Q, Buchwald SL. Tetrahedron 2009;65:6576.

6. For additional examples of amidations with aryl chlorides, see: (a) Ghosh A, Sieser JE, Riou M, Cai W, Rivera-Ruiz L. Org Lett 2003;5:2207. [PubMed: 12816410] (b) Shen Q, Shekhar S, Stambuli JP, Hartwig JF. Angew Chem, Int Ed 2005;44:1371. (c) Ligthart GBWL, Ohkawa H, Sijbesma RP, Meijer EW. J Org Chem 2006;71:375. [PubMed: 16388663] (d) Piguel S, Legraverend M. J Org Chem 2007;72:7026. [PubMed: 17685576] (e) McLaughlin M, Palucki M, Davies IW. Org Lett 2006;8:3311. [PubMed: 16836393] For an example of amidation with gem-dichloroolefins, see: (f) Ye W, Mo J, Zhao T, Xu B. Chem Commun 2009:3246.

7. For intramolecular examples, see: (a) Wolfe JP, Rennels RA, Buchwald SL. Tetrahedron 1996;52:7525. (b) Wagaw S, Rennels RA, Buchwald SL. J Am Chem Soc 1997;119:8451. (c) Yang BH, Buchwald SL. Org Lett 1999;1:35. [PubMed: 10822529] (d) Yamada K, Kubo T, Tokuyama H, Fukuyama T. Synlett 2002:231. (e) Ooi T, Kameda M, Maruoka K. J Am Chem Soc 2003;125:5139. [PubMed: 12708866] (f) Poondra RR, Turner NJ. Org Lett 2005;7:863. [PubMed: 15727460] (g) Bonnaterre F, Bois-Choussy M, Zhu J. Org Lett 2006;8:4351. [PubMed: 16956224] (h) Hoogenbrand A, Lange JHM, Iwema-Bakker WI, Hartog JAJ, Schaik J, Feenstra RW, Terpstra JW. Tetrahedron Lett 2006;47:4361. (i) Feng G, Wu J, Dai W. Tetrahedron Lett 2007;48:401. (j) Hoogenbrand A, Lange JHM, Hartog JAJ, Henzen R, Terpstra JW. Tetrahedron Lett 2007;48:4461. (k) Furuta T, Kitamura Y, Hashimoto A, Fujii S, Tanaka K, Kan T. Org Lett 2007;9:183. [PubMed: 17217260] (l) Kalinski C, Umkehrer M, Ross G, Kolb J, Burdack C, Hiller W. Tetrahedron Lett 2006;47:3423.

8. For isolated intermolecular examples, see: Refs 2c, 3a, 3b, 5a, and Deng W, Wang YF, Zou Y, Liu L, Guo QX. Tetrahedron Lett 2004;45:2311.

9. For secondary formamides, see: Refs 2c, 3a, 3b, 4c, 5a.

10. (a) Wagner J, Wagner ML, Hening WA. Ann Pharmacother 1998;36:680. [PubMed: 9640488] (b) VanBever WFM, Niemegeers CJE, Janssen PAJ. J Med Chem 1974;17:1047. [PubMed: 4420811] (c) Anderson, R.; Hokama, T.; Lee, S-F.; Oey, R.; Elich, T.; Breazeale, S. Preparation of modulators of acetyl coenzyme A carboxylase as fungicides and pharmaceuticals. U.S. Pat. 20080200461. 2008.

11. Greene, TW.; Wuts, PGM. Protective Groups in Organic Chemistry. Vol. 3. John Wiley & Sons; New York: 1999. p. 503-564.

12. Fors BP, Watson DA, Biscoe MR, Buchwald SL. J Am Chem Soc 2008;130:13552. [PubMed: 18798626]

13. Sergeev AG, Artamkina GA, Beletskaya IP. Tetrahedron Lett 2003;44:4719.

14. For a more complete ligand examination and condition optimization, see Supporting Information.

15. Aryl nonaflates can be easily prepared from the corresponding phenols and nonafluorobutanesulfonyl fluoride. For their preparation and use in C–N coupling, see: (a) Anderson KW, Mendez-Perez M, Priego J, Buchwald SL. J Org Chem 2003;68:9563. [PubMed: 14656080] (b) Tundel RE, Anderson KW, Buchwald SL. J Org Chem 2006;71:430. [PubMed: 16388678]

16. For the use of ArONf substrates in Heck reactions, see: (a) Beletskaya IP, Cheprakov AV. Chem Rev 2000;100:3009. [PubMed: 11749313] (b) Lyapkalo IM, Webel M, Reibig HU. Eur J Org Chem 2002:3646.

17. Aryl nonaflates are generally more resistant to hydrolysis than the corresponding triflates. For an example, see: Zhang X, Sui Z. Tetrahedron Lett 2003;44:3071.

18. Anderson KW, Ikawa T, Tundel RE, Buchwald SL. J Am Chem Soc 2006;128:10694. [PubMed: 16910660]

xix. Coordination of dba can result in diminished reactivity. See: (a) Fairlamb IJS, Kapdi AR, Lee AF, McGlacken GP, Weissburger F, de Vries AHM, Vondervoort LS. Chem Eur J 2006;12:8750. (b) Mace Y, Kapdi AR, Fairlamb IJS, Jutand A. Organometallics 2006;25:1795. (c) Amatore C, Jutand A. Coord Chem Rev 1998;178:511.

xx. For Cu-catalyzed arylations of N-aryl amides with aryl iodides and bromides: Refs 2b, c, f and Freeman HS, Butler JR, Freedman LD. J Org Chem 1978;43:4975.

xxi. Yin J, Buchwald SL. unpublished results.

xxii. For isolated examples of N-arylation with secondary carbamates, see: Refs 3a, 3c and Tasler S, Mies J, Lang M. Adv Synth Catal 2007;349:2286.

xxiii. (a) Littke AF, Fu GC. Angew Chem, Int Ed 2002;41:4176. (b) Grushin VV, Alper H. Chem Rev 1994;94:1047.

xxiv. For Cu-catalyzed di-arylations with aryl bromides and iodides, see: (a) HisayukiKHiroyukiMKojiHMethod for Producing Aromatic Diamine DerivativeEP 15936652005 (b)YabunouchiNKawamuraMAromatic Amine Derivative and Organic Electroluminescent Device Using the SameWO20060730542006(c)KawamuraHYabunouchiNAromatic Triamine Compound and Organic Electroluminescent Device Using the SameWO20061149212006

xxv. Dalton, J.; Barrett, C.; He, Y.; Hong, S.; Miller, DD.; Mohler, ML.; Narayanan, R.; Wu, Z. Nuclear Receptor Binding Agents. WO 2007/062230 A2. 2007.

xxvi. Fujii Y, Shimada T, Koike T, Hosaka K, Tabei K, Namatame T, Tajima A, Yoneda M, Terano A, Hiraishi H. Aliment Pharmacol Ther Symp Ser 2006;2:285.

xxvii. Richens DT. Chem Rev 2005;105:1961. [PubMed: 15941207]

28. For representative examples, see: (a) Ariafard A, Lin Z. Organometallics 2006;25:4030. (b) Legault CY, Garcia Y, Merlic CA, Houk KN. J Am Chem Soc 2007;129:12664. [PubMed: 17914827] (c) Nova A, Ujaque G, Maseras F, Lledós A, Espinet P. J Am Chem Soc 2006;128:14571. [PubMed: 17090041] (d) Álvarez R, Faza ON, López CS, de Lera AR. Org Lett 2006;8:35. [PubMed: 16381561] (e) Braga AAC, Ujaque G, Maseras F. Organometallics 2006;25:3647. (f) Ananikov VP, Musaev DG, Morokuma K. Organometallics 2005;24:715. (g) Zuidema E, van Leeuwen PWNM, Bo C. Organometallics 2005;24:3703.

29. For examples that illustrate the importance of calculating the full ligand structure in Pd-catalyzed cross-coupling reactions, see: (a) Li Z, Fu Y, Guo Q, Liu L. Organometallics 2008;27:4043. (b) Barder TE, Biscoe MR, Buchwald SL. Organometallics 2007;26:2183.

30. For the calculated effect of ligand structure on the barrier to oxidative addition of aryl halides with $L_nPd(0)$, see: Ref 28a and (a) Kozuch S, Amatore C, Jutand A, Shaik S. Organometallics 2005;24:2319.For the effect on the overall cycle of a Pd-catalyzed Suzuki–Miyuara coupling, see: (b) Huang Y, Weng C, Hong F. Chem Eur J 2008;14:4426.For the effect on the barrier to reductive elimination of $L_nPd(II)ArX$ complexes, see: Ref 28g and (c) Ananikov VP, Musaev DG, Morokuma K. Eur J Inorg Chem 2007:5390. (d) Ariafard A, Yates BF. J Organomet Chem 2009;694:2075.For the effect on the overall cycle of Cu-catalyzed amide arylations, see: (e) Zhang S, Liu L, Fu Y, Guo Q. Organometallics 2007;26:4546.

xxxi. For computational studies on Rh/xantphos complexes and their behavior in hydroformylation reactions, see: (a) Landis CR, Uddin J. Dalton Trans 2002:729. (b) van der Veen LA, Keeven PH, Schoemaker GC, Reek JNH, Kamer PCJ, van Leeuwen PWNM, Lutz M, Spek AL. Organometallics 2000;19:872.

32. Frisch, MJ.; Trucks, GW.; Schlegel, HB.; Scuseria, GE.; Robb, MA.; Cheeseman, JR.; Montgomery, JA., Jr; Vreven, T.; Kudin, KN.; Burant, JC.; Millam, JM.; Iyengar, SS.; Tomasi, J.; Barone, V.; Mennucci, B.; Cossi, M.; Scalmani, G.; Rega, N.; Petersson, GA.; Nakatsuji, H.; Hada, M.; Ehara, M.; Toyota, K.; Fukuda, R.; Hasegawa, J.; Ishida, M.; Nakajima, T.; Honda, Y.; Kitao, O.; Nakai, H.; Klene, M.; Li, X.; Knox, JE.; Hratchian, HP.; Cross, JB.; Bakken, V.; Adamo, C.; Jaramillo, J.; Gomperts, R.; Stratmann, RE.; Yazyev, O.; Austin, AJ.; Cammi, R.; Pomelli, C.; Ochterski, JW.; Ayala, PY.; Morokuma, K.; Voth, GA.; Salvador, P.; Dannenberg, JJ.; Zakrzewski, VG.; Dapprich, S.; Daniels, AD.; Strain, MC.; Farkas, O.; Malick, DK.; Rabuck, AD.; Raghavachari, K.; Foresman, JB.; Ortiz, JV.; Cui, Q.; Baboul, AG.; Clifford, S.; Cioslowski, J.; Stefanov, BB.; Liu, G.; Liashenko, A.; Piskorz, P.; Komaromi, I.; Martin, RL.; Fox, DJ.; Keith, T.; Al-Laham, MA.; Peng, CY.; Nanayakkara, A.; Challacombe, M.; Gill, PMW.; Johnson, B.; Chen, W.; Wong, MW.; Gonzalez, C.; Pople, JA. Gaussian 03, Revision D.01. Gaussian, Inc; Wallingford CT: 2004.

33. Hay PJ, Wadt WR. J Chem Phys 1985;82:299.

34. Cossi M, Rega N, Scalmani G, Barone V. J Comp Chem 2003;24:669. [PubMed: 12666158]

35. Boys SF, Bernardi F. Mol Phys 1970;19:553.

36. For instances where the correction of BSSE is important in theoretical studies of Pd-catalyzed processes, see: (a) Frankcombe KE, Cavell KJ, Yates BF, Knott RB. J Phys Chem 1996;100:18363. (b) Delbecq F, Lapouge C. Organometallics 2000;19:2716. (c) de Jong GT, Sola M, Visscher L, Bickelhaupt FM. J Chem Phys 2004;121:9982. [PubMed: 15549873]

37. (a) Birkholz MN, Freixa Z, van Leeuwen PWNM. Chem Soc Rev 2009;38:1099. [PubMed: 19421583] (b) Kamer PCJ, van Leeuwen PWNM, Reek JNH. Acc Chem Res 2001;34:895. [PubMed: 11714261]

38. For the cross coupling of activated aryl chlorides using a Pd/xantphos catalyst, see: Refs 6c,d and (a) Itoh T, Mase T. Org Lett 2004;6:4587. [PubMed: 15548082] (b) Patriciu OI, Finaru AL, Massip S, Léger JM, Jarry C, Guillaumet G. Eur J Org Chem 2009:3753.

39. Xantphos-Pd(II) complexes are often most stable as the trans isomer, see: Ref 3b and (a) Zuideveld MA, Swennenhuis BHG, Boele MDK, Guari Y, van Strijdonck GPF, Reek JNH, Kamer PCJ, Goubitz K, Fraanje J, Lutz M, Spek AL, van Leeuwen PWNM. Dalton Trans 2002:2308. (b) Fujita K, Yamashita M, Puschmann F, Alvarez-Falcon MM, Incarvito CD, Hartwig JF. J Am Chem Soc 2006;128:9044. [PubMed: 16834372]

40. Barder TE, Walker SD, Martinelli JM, Buchwald SL. J Am Chem Soc 2005;127:4685. [PubMed: 15796535]

41. For experimentally-determined binding energies of amines and anilines with dimeric SPhos·Pd(II)(Ar)(Cl) complexes, see: Biscoe MR, Barder TE, Buchwald SL. Angew Chem, Int Ed 2007;46:7232.

42. (a) Deeth RJ, Smith A, Brown JM. J Am Chem Soc 2004;126:7144. [PubMed: 15174886] and references cited therein. (b) Tanaka D, Romeril SP, Myers AG. J Am Chem Soc 2005;127:10323. [PubMed: 16028944]

43. Guari Y, van Strijdonck GPF, Boele MDK, Reek JNH, Kamer PCJ, van Leeuwen PWNM. Chem Eur J 2001;7:475.

44. Howells RD, McCown JD. Chem Rev 1977;77:69.

xlv. Wadt WR, Hay J. J Chem Phys 1985;82:284.

46. Hartwig JF. Inorg Chem 2007;46:1936. [PubMed: 17348724]

47. For a computational study on the reductive elimination of aryl amines from biaryl monophosphine arylpalladium amido complexes, see: Barder TE, Buchwald SL. J Am Chem Soc 2007;129:12003. [PubMed: 17850080]

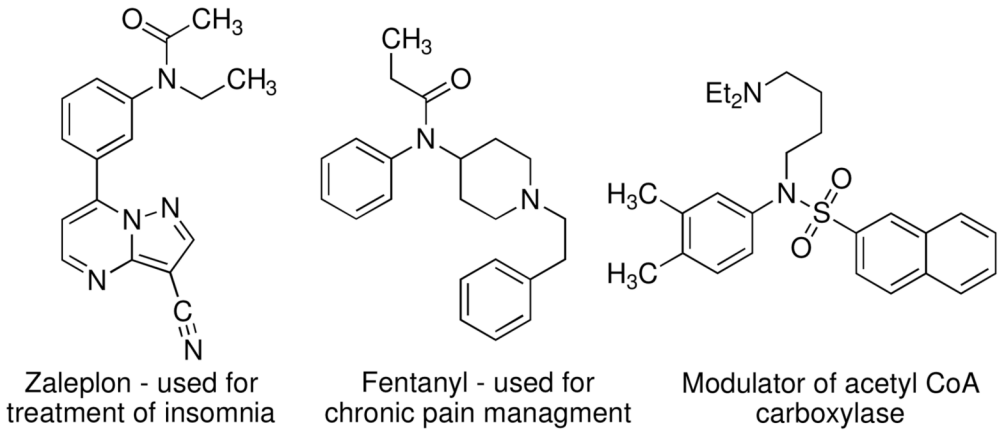

Figure 1.
Representative Biologically Active Tertiary Aryl Amides and Sulfonamides.

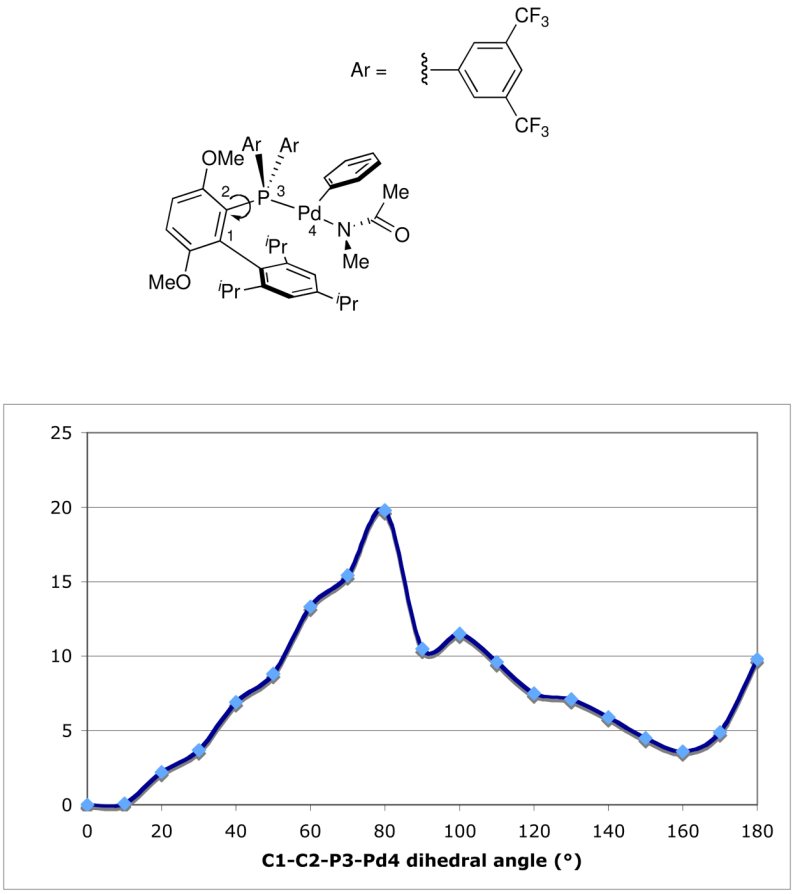

Figure 2.
Potential Energy Scan for Rotation About the C2–P3 Bond.

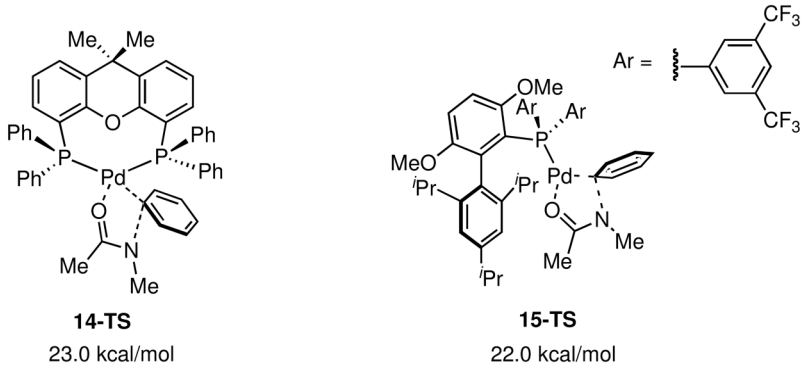

Figure 3.
Five-Membered Cyclic Transition States for Reductive Elimination.

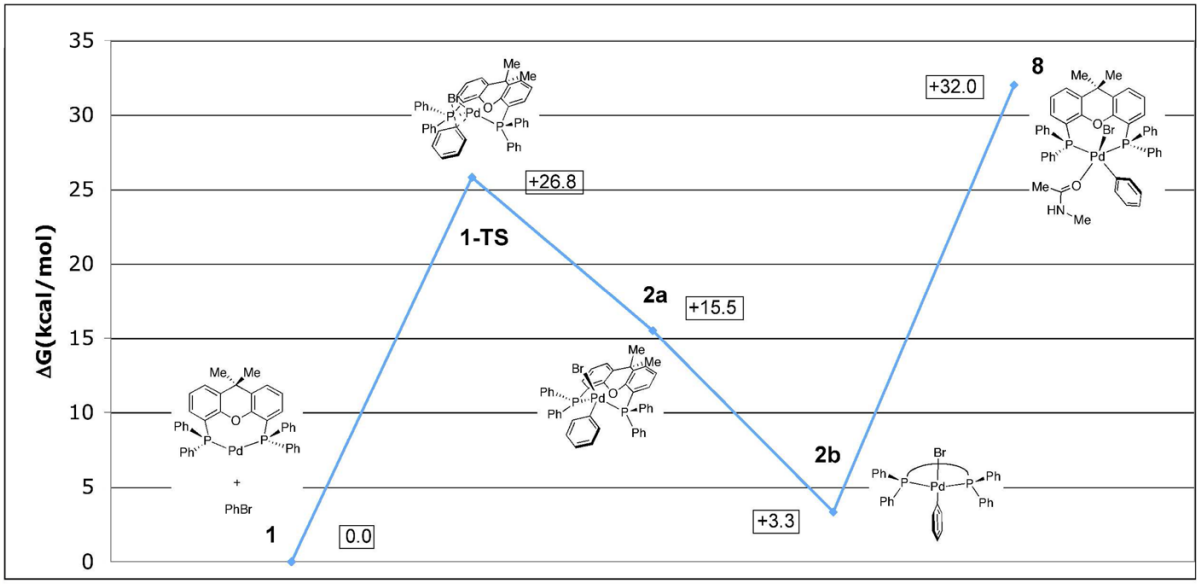

Figure 4.
Partial Potential Energy Diagram of the Catalytic Cycle with the xantphos-Pd catalyst.

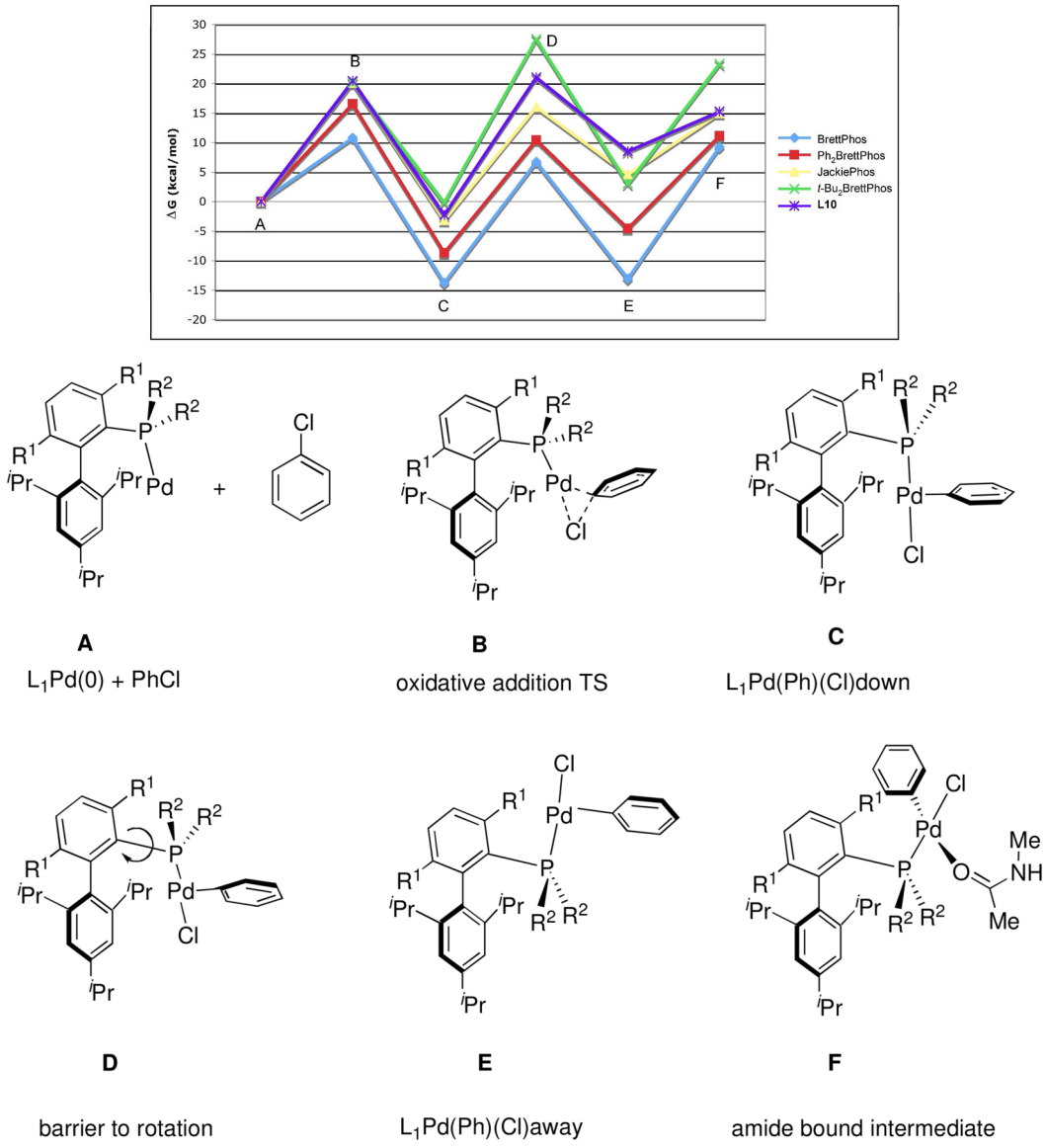

Figure 5.
Partial Potential Energy Diagram of the Catalytic Cycle with biarylmonophosphine-Pd Catalysts.

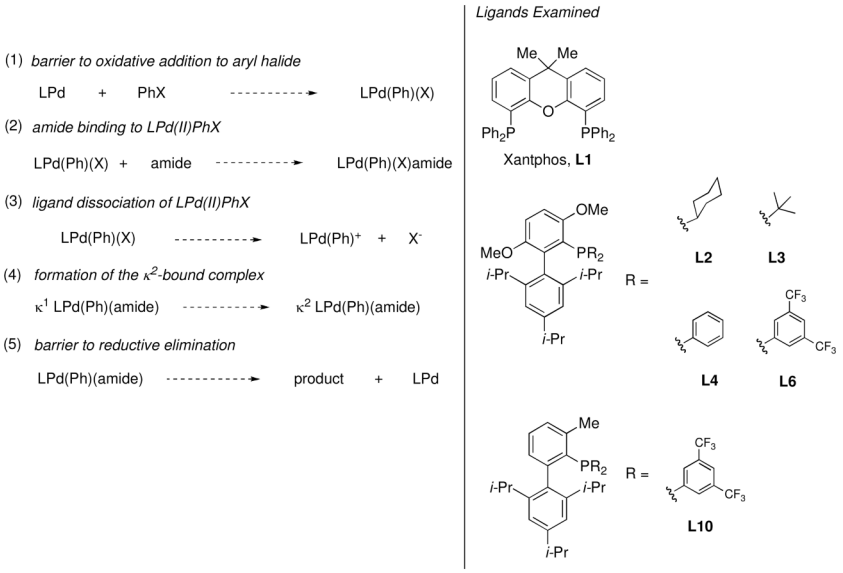

Scheme 1.
Processes Examined in Our Computational Studies.

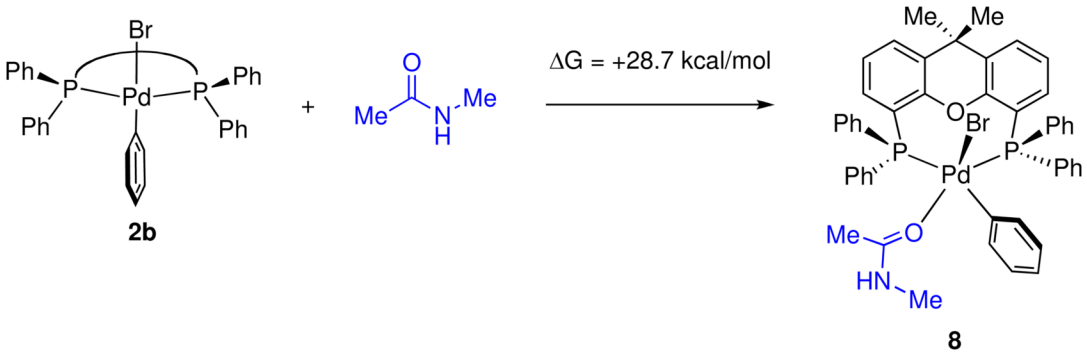

Scheme 2.
Calculated Binding Energy of *N*-Methyl Acetamide to xantphos·Pd(Ph)(Br).

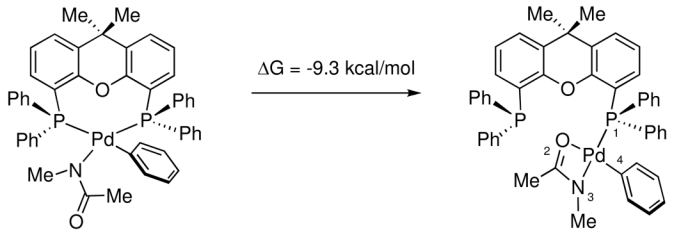

19 20

Bond Angles (deg)		Bond Lengths (Å)	
P1–Pd–O2	106.0	P1–Pd	2.32
O2–Pd–N3	60.7	O2–Pd	2.27
N3–Pd–C4	98.8	N3–Pd	2.11
C4–Pd–P1	94.4	C4–Pd	2.01

Scheme 3.
Calculated Energy for κ^2-Binding of xantphos·Pd(Ph)(amidate).

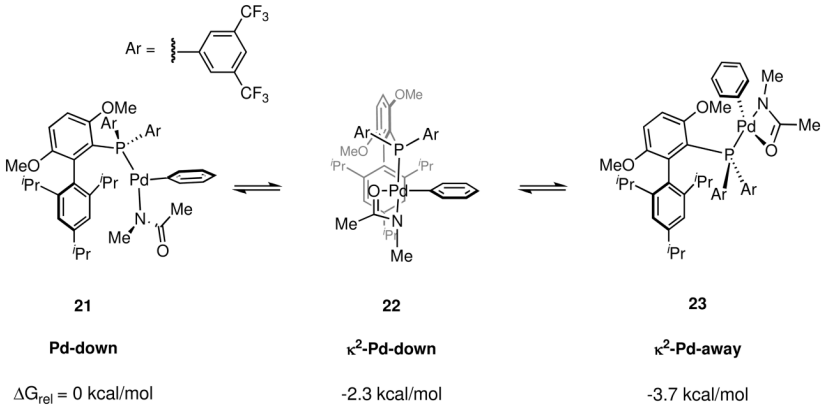

Scheme 4.
Calculated Energies of κ^2-Binding of JackiePhos·Pd(Ph)(amidate).

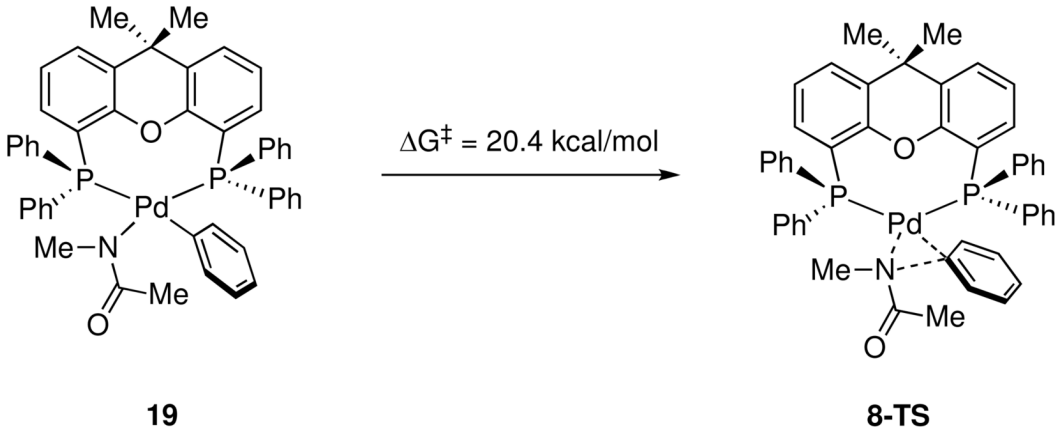

19 **8-TS**

Scheme 5.
Calculated Barrier for Reductive Elimination of *cis*-xantphos·Pd(Ph)(amidate).

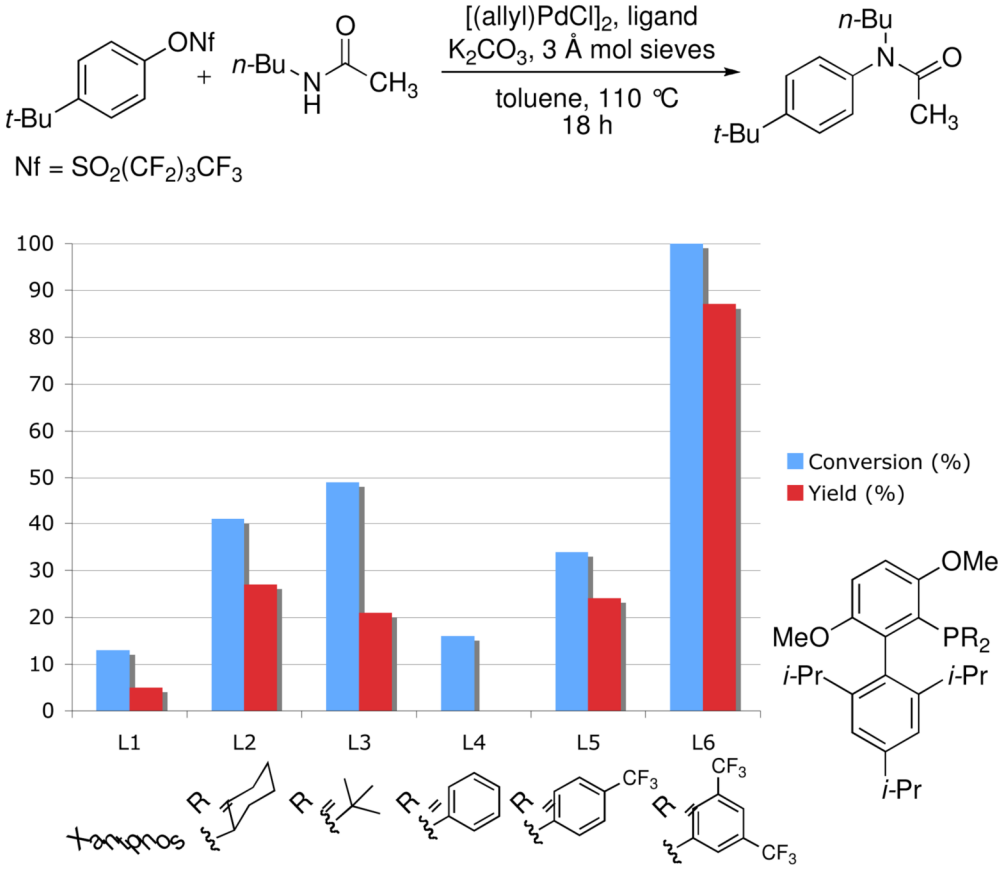

Chart 1.

Ligand Optimization for the Coupling of 4-*t*-butylphenyl nonaflate and *N*-butyl acetamide.[a]

[a] ArONf (1 equiv), amide (2.5 equiv), $[(allyl)PdCl]_2$ (1 mol%), ligand (5 mol%), base (2.0 equiv), 3 Å mol sieves (50 mg/ml), solvent (0.25 M), 110 °C, 18 h.

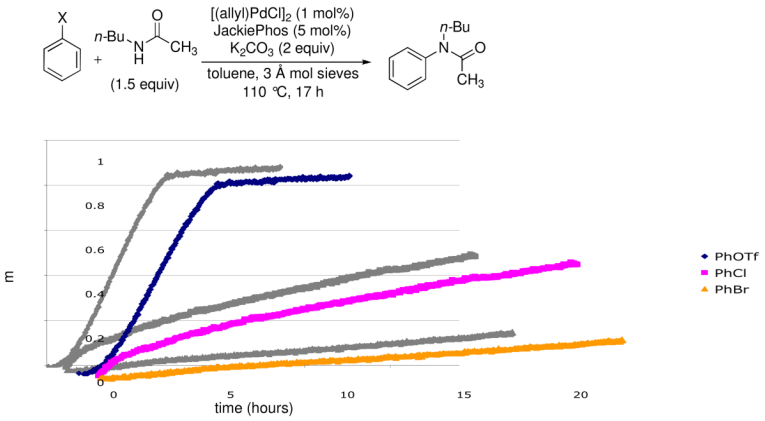

Chart 2.
Comparison of Reaction Profiles for PhOTf, PhCl, and PhBr.

Table 1

Pd-Catalyzed Coupling of Aryl Nonaflates and Triflates with Secondary Amides.[a]

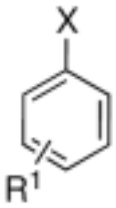

entry	ArX
	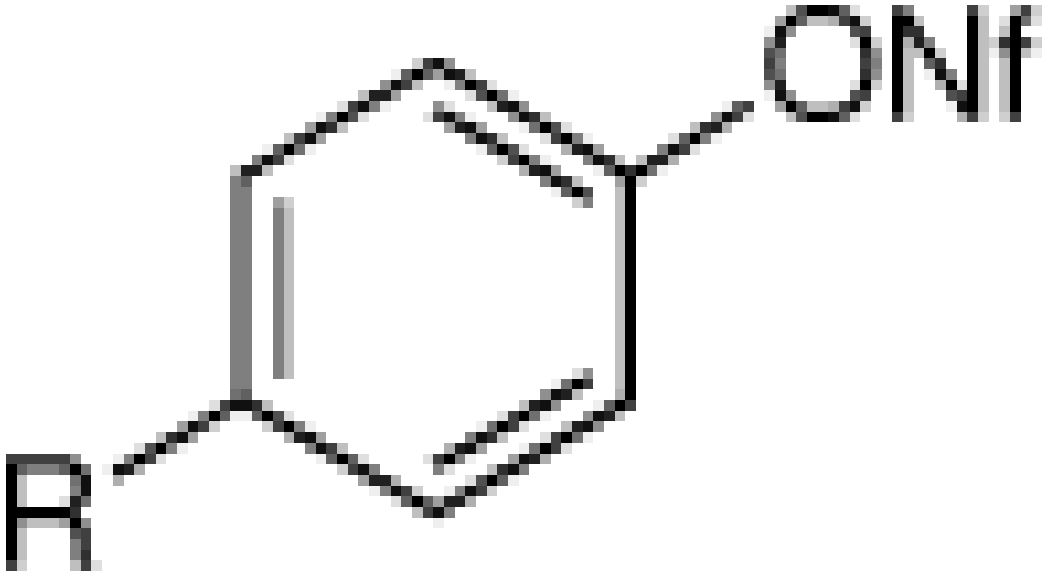
1	R = *t*-Bu
2	R = Me
3	R = CO_2Me

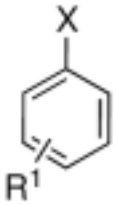

entry	ArX
4	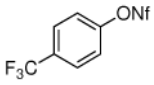

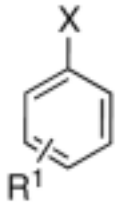

entry	ArX
5	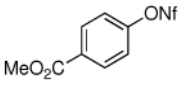

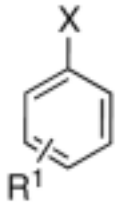

entry	ArX
6[c]	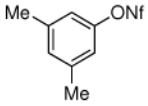

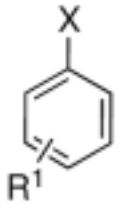

entry	ArX
7	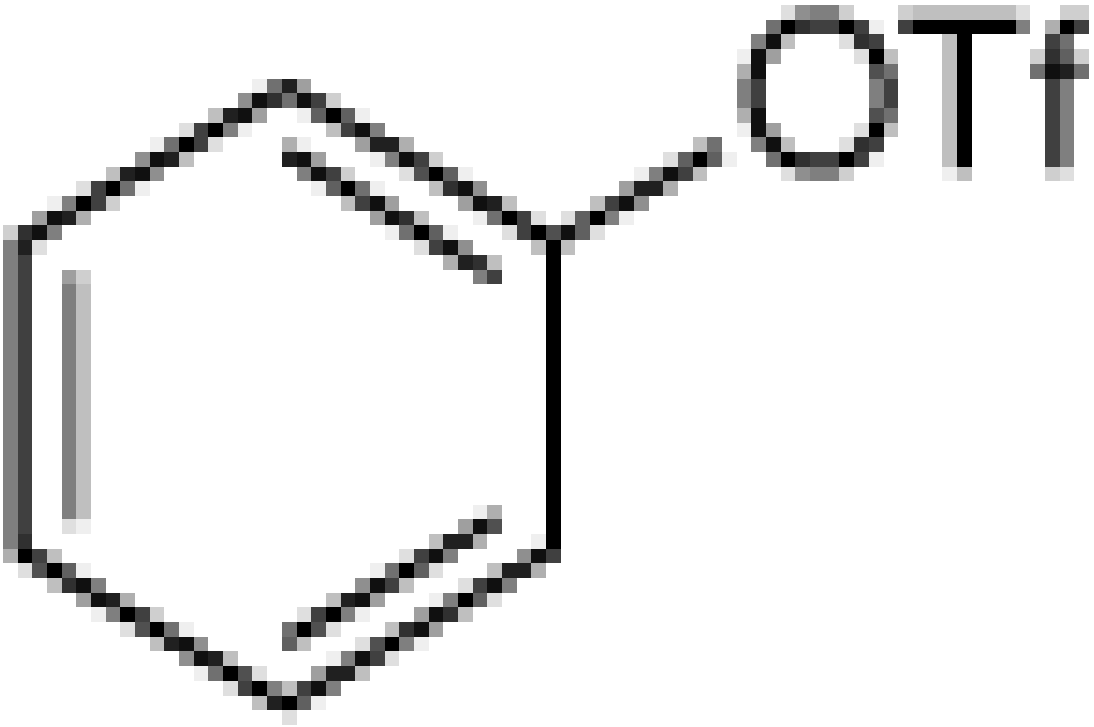

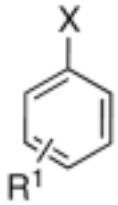

entry	ArX
8	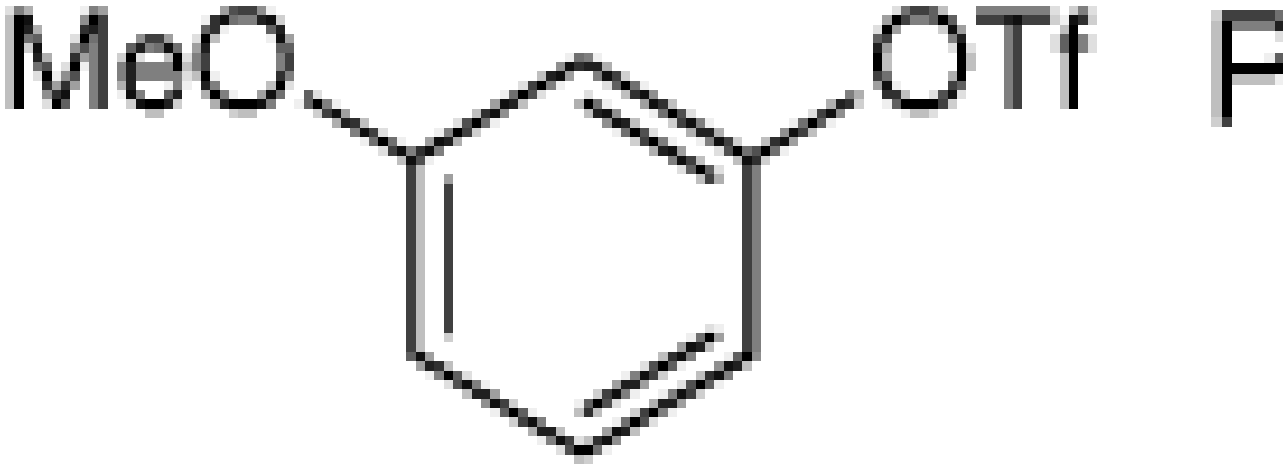

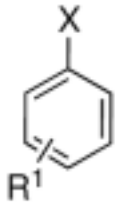

entry	ArX
9	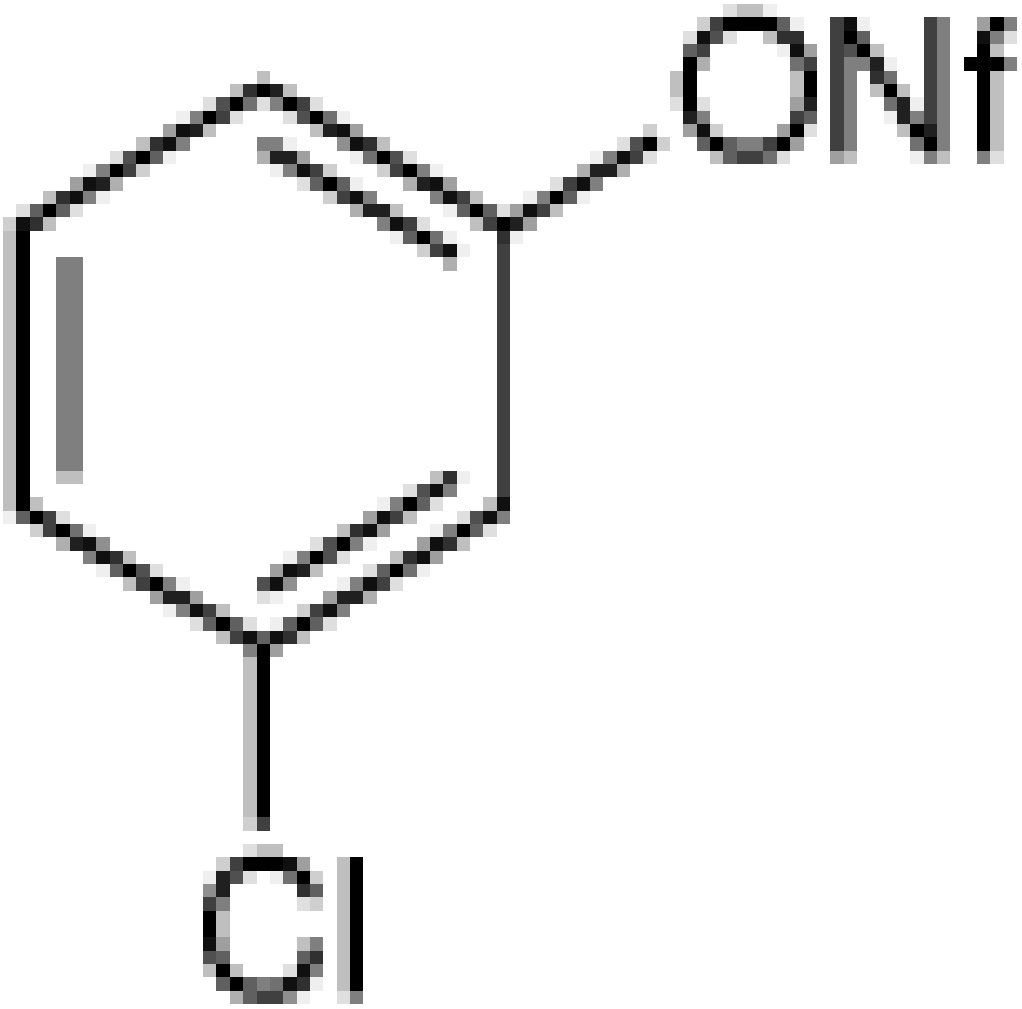

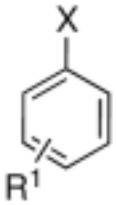

entry	ArX
10	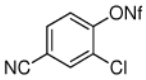

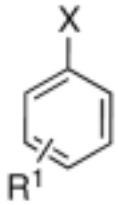

entry	ArX
11[d]	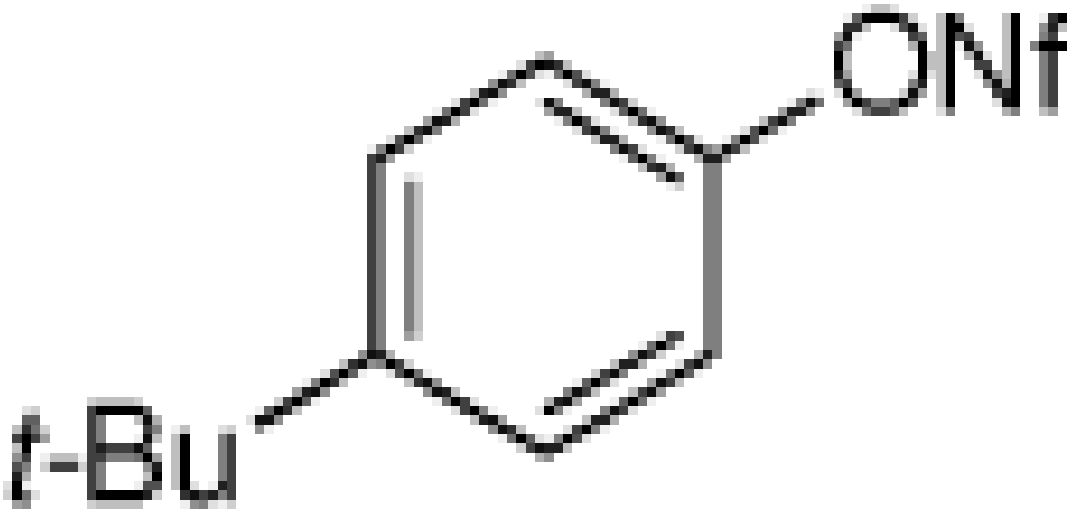

[a] Reaction conditions: ArONf/ArOTf (1 equiv), amide (2.5 equiv), $[(allyl)PdCl]_2$ (1 mol%), JackiePhos (5 mol%), K_2CO_3 (2.0 equiv), 3 Å mol sieves (200 mg/mmol), toluene (0.25 M), 110 °C, 17 h.

[b] Yields reported are an average of at least two runs determined to be >95% pure by elemental analysis or ^{1}H NMR.

[c] $Pd(OAc)_2$ (3 mol%), JackiePhos (7 mol%), H_2O activation

[d] K_3PO_4 was used instead of K_2CO_3.

Table 2

Pd-Catalyzed Coupling of Aryl Nonaflates and Triflates with Secondary Ureas, Carbamates, and Sulfonamides.[a]

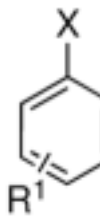

entry	ArX
1	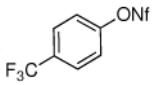

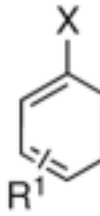

entry	ArX
2	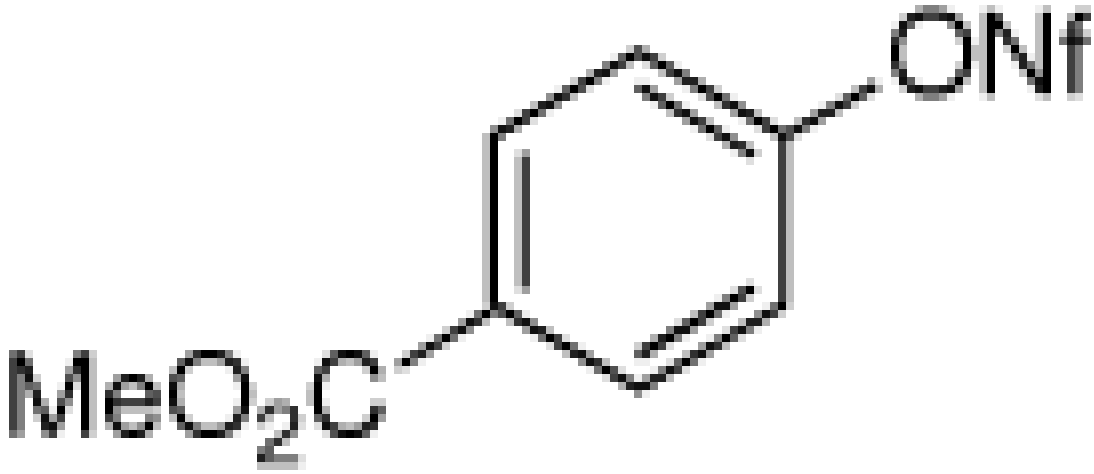

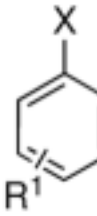

entry	ArX
3	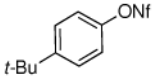

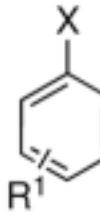

entry	ArX
4	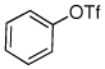

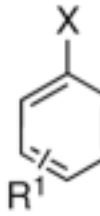

entry	ArX
5	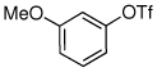

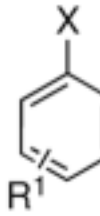

entry	ArX
6	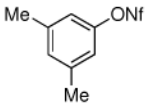

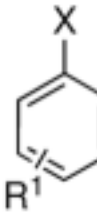

entry	ArX
7	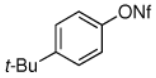

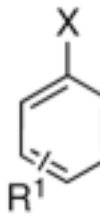

entry	ArX
8	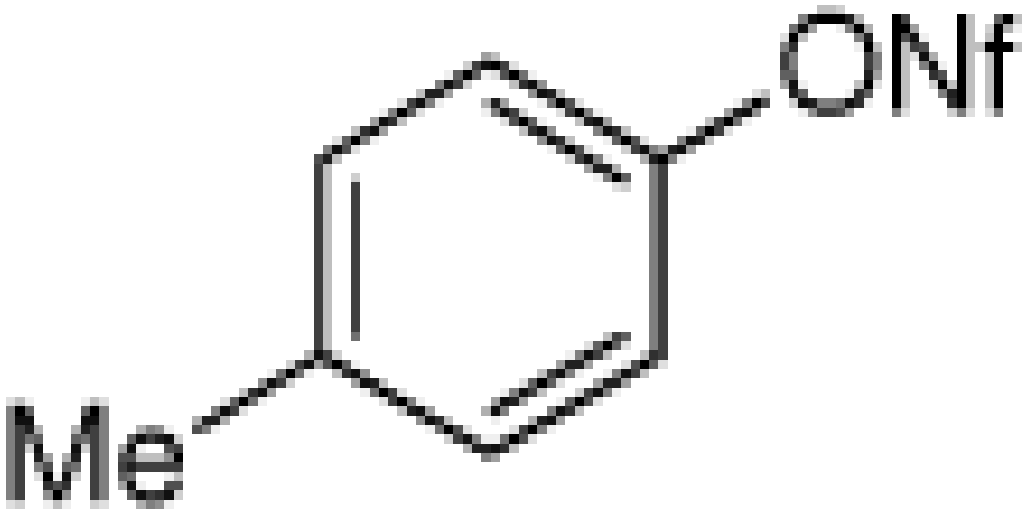

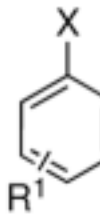

entry	ArX
9	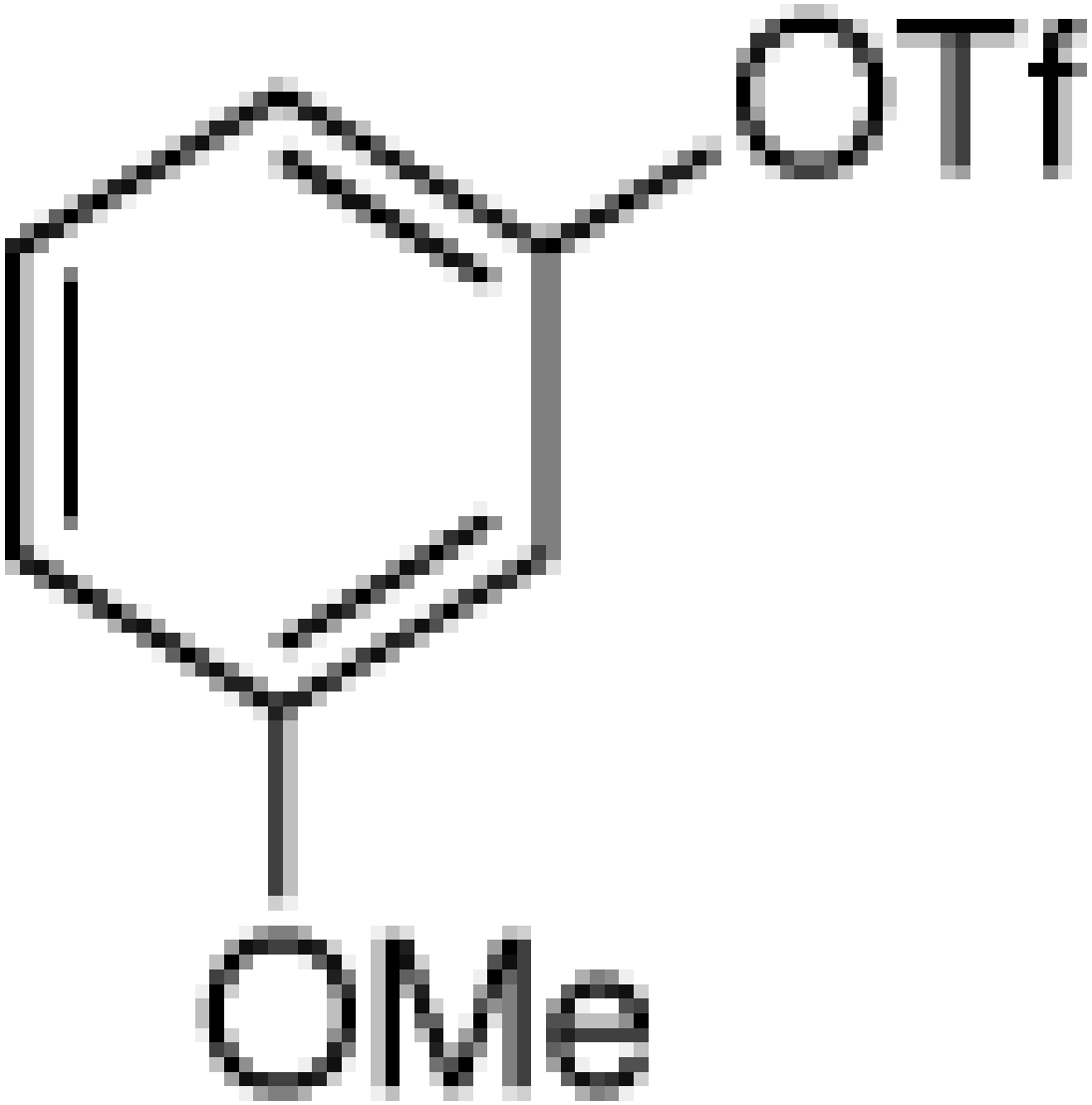

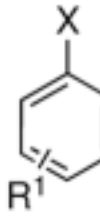

entry	ArX
10	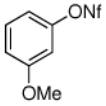

[a] Reaction conditions: ArONf/ArOTf (1 equiv), urea or carbamate (2.5 equiv), $[(allyl)PdCl]_2$ (1 mol%), JackiePhos (5 mol%), K_2CO_3 (2.0 equiv), 3 Å mol sieves (50 mg/ml), toluene (0.25 M), 110 °C, 17 h.

[b] Yields reported are an average of at least two runs determined to be >95% pure by elemental analysis or ^1H NMR.

Table 3

Pd-Catalyzed Coupling of Aryl Chlorides with Secondary Amides, Carbamates, and Sulfonamides.[a]

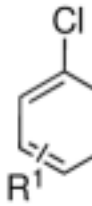

entry	ArCl
1	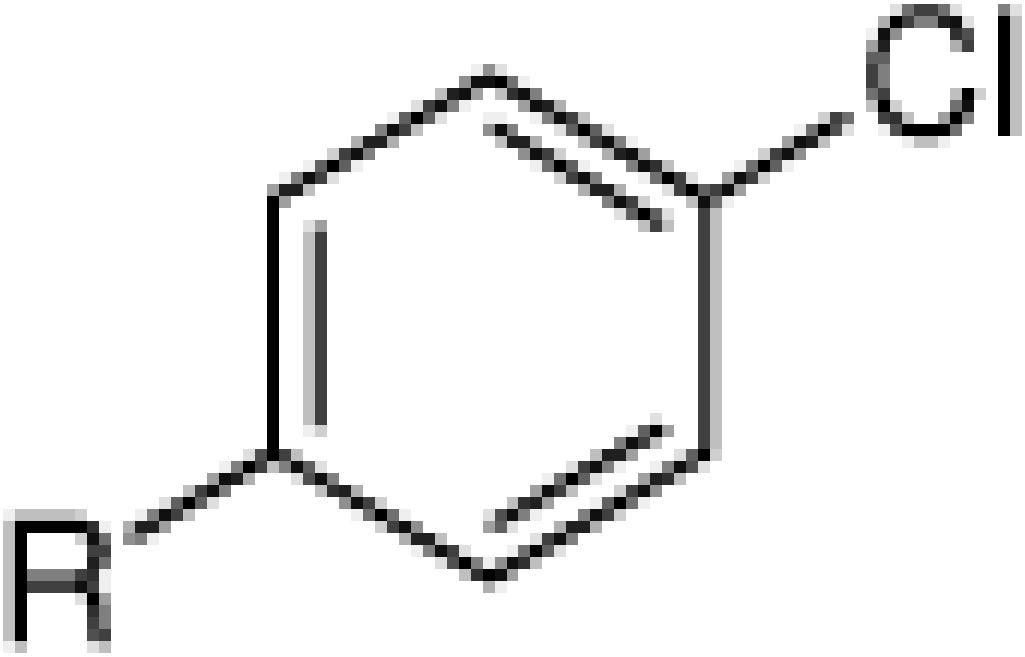 R = *t*-Bu
2	R = *n*-Bu

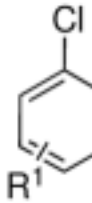

entry	ArCl
3	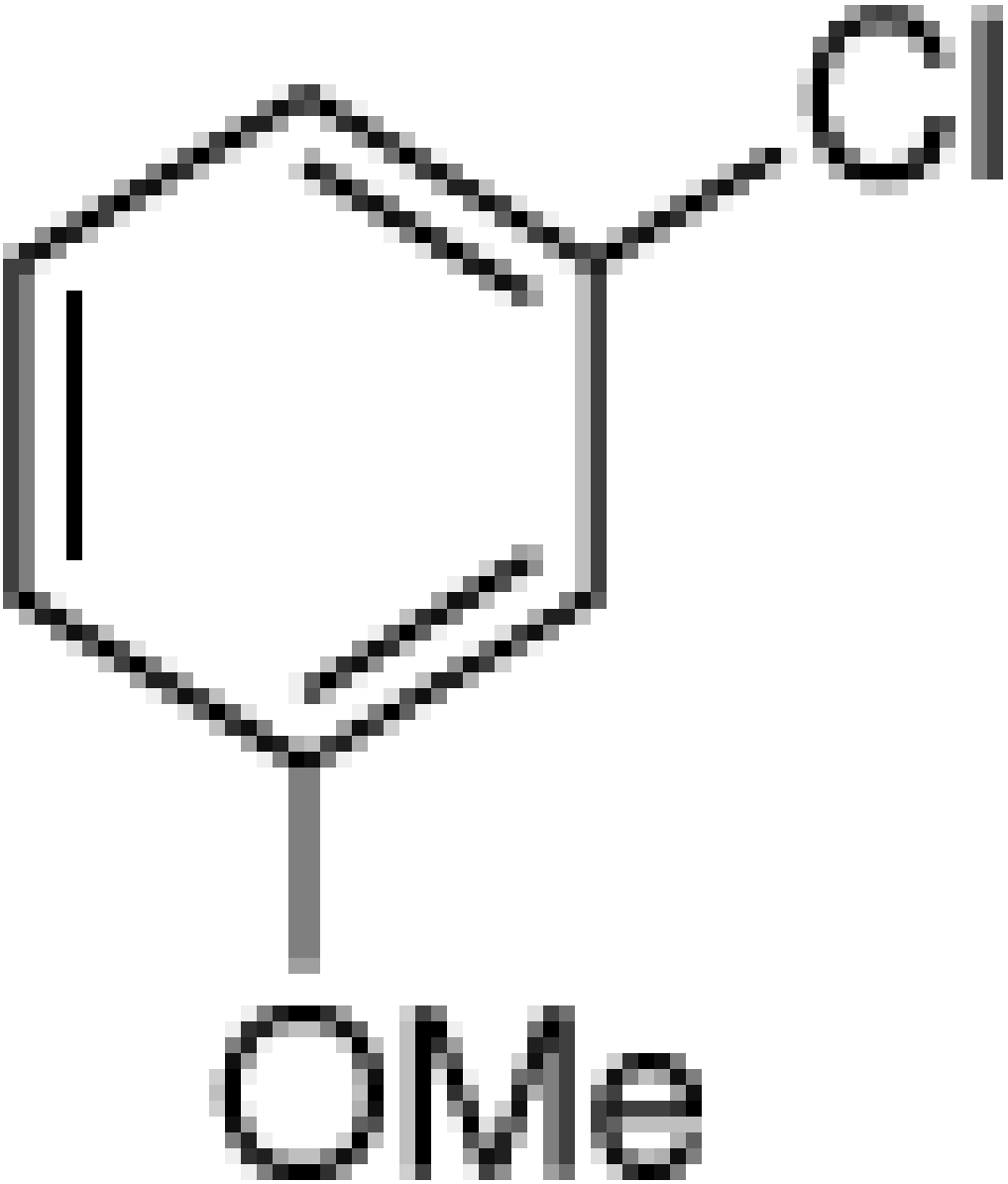

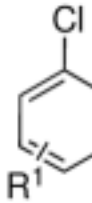

entry	ArCl
4	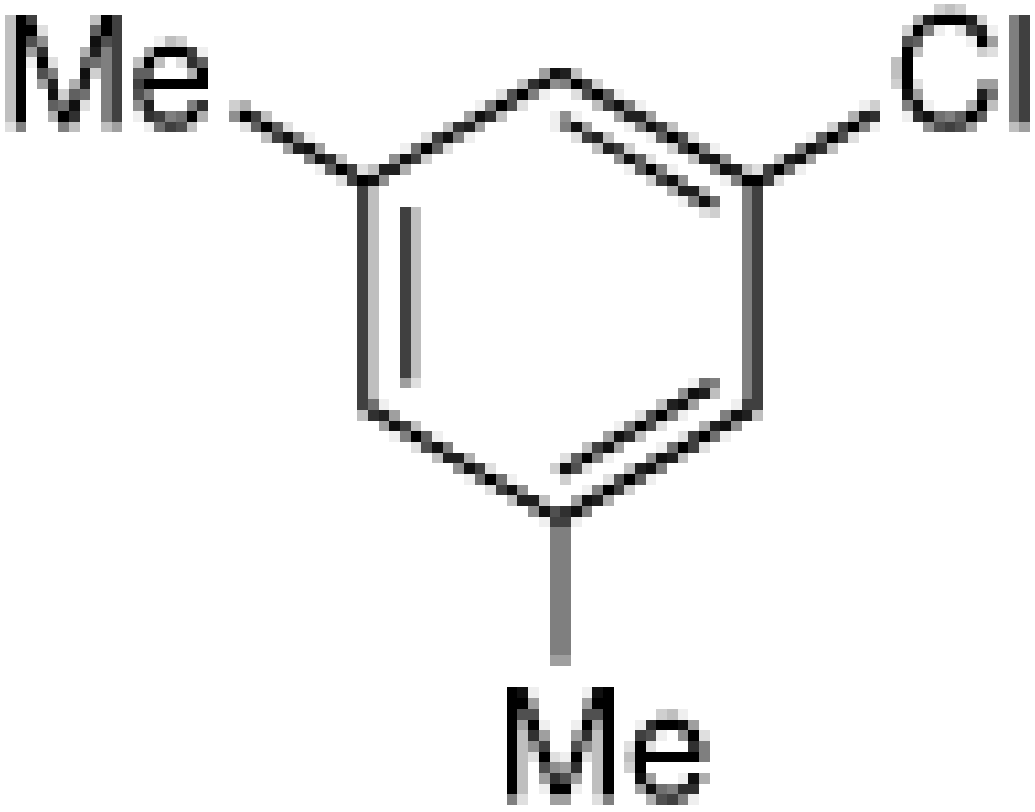

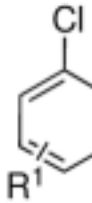

entry	ArCl
5	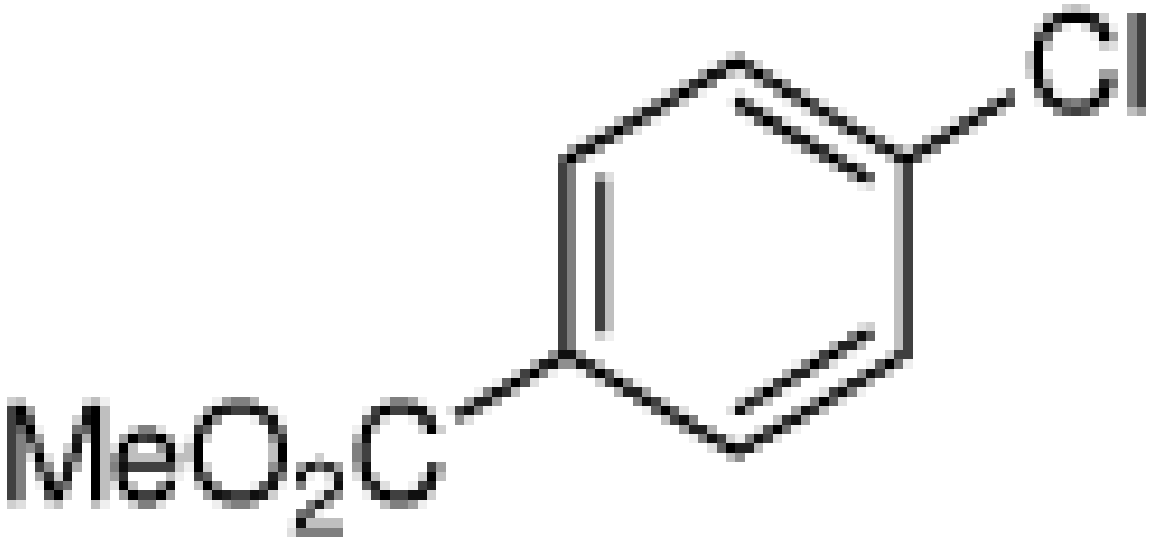

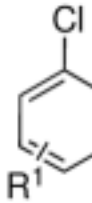

entry	ArCl
6[c]	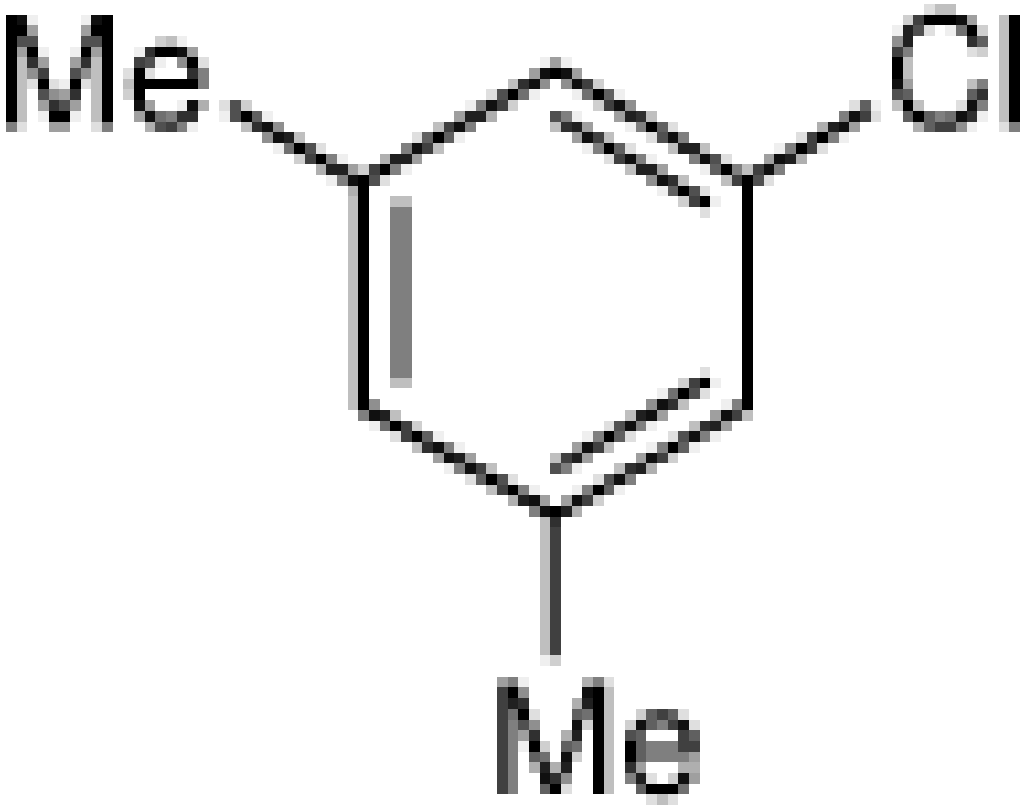

[a] Reaction conditions: ArCl (1 equiv), amide (2.5 equiv), $[(allyl)PdCl]_2$ (1 mol%), JackiePhos (5 mol%), base (2.0 equiv), 3 Å mol sieves (200 mg/mmol), solvent (0.25 M), 110 °C, 18 h.

[b] Yields reported are an average of at least two runs determined to be >95% pure by elemental analysis or ^1H NMR.

[c] K_3PO_4 was used instead of Cs_2CO_3.

Table 4

Diarylation of Primary Amides and Synthesis of Nuclear Receptor Binding Agent and Related Analogs.[a,b]

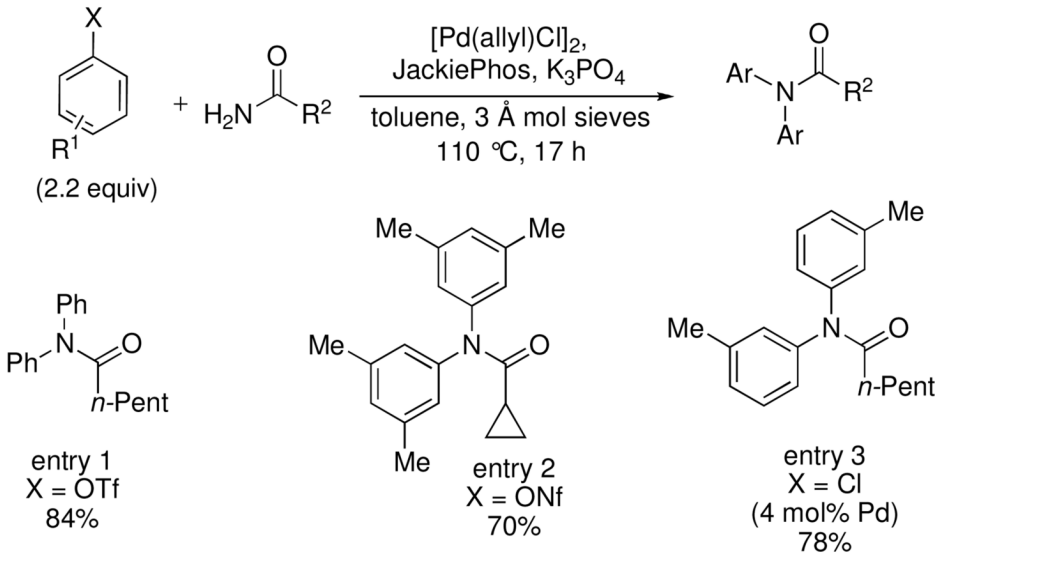

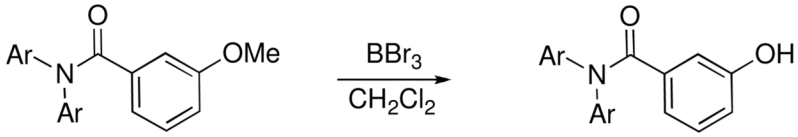

entry	X	Ar	Yield[c]
4	OTf	Ph	67%
5	ONf	*p*-CF_3Ph	70%
6	ONf	*m*-OMe	54%

Ar = Ph 82%

- Nuclear Receptor Binding Agent

[a]Reaction conditions: ArX (2.2 equiv), amide (1.0 equiv), $[(allyl)PdCl]_2$ (1 mol%), JackiePhos (5 mol%), K_3PO_4 (3.0 equiv), 3 Å mol sieves (200 mg/mmol), toluene (0.25 M), 110 °C, 17 h.

[b]Yields reported are an average of at least two runs determined to be >95% pure by elemental analysis or ^{1}H NMR.

[c]Runs conducted with $[(allyl)PdCl]_2$ (1.5 mol%), JackiePhos (7 mol%), 42 h.

Table 5

Variation of the Upper Ring of the Biaryl Backbone

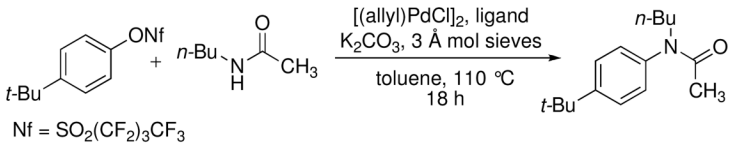

Nf = $SO_2(CF_2)_3CF_3$

entry	ligand	conversion (%)	yield (%)
1	**L6**	100	87
2	**L7**	20	5
3	**L8**	3	0
4	**L9**	100	83

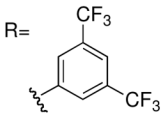

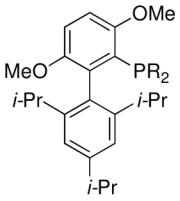

L6, JackiePhos

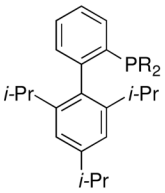

L7

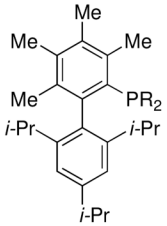

L8

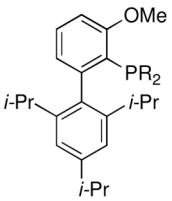

L9

Table 6

Competition Experiments.

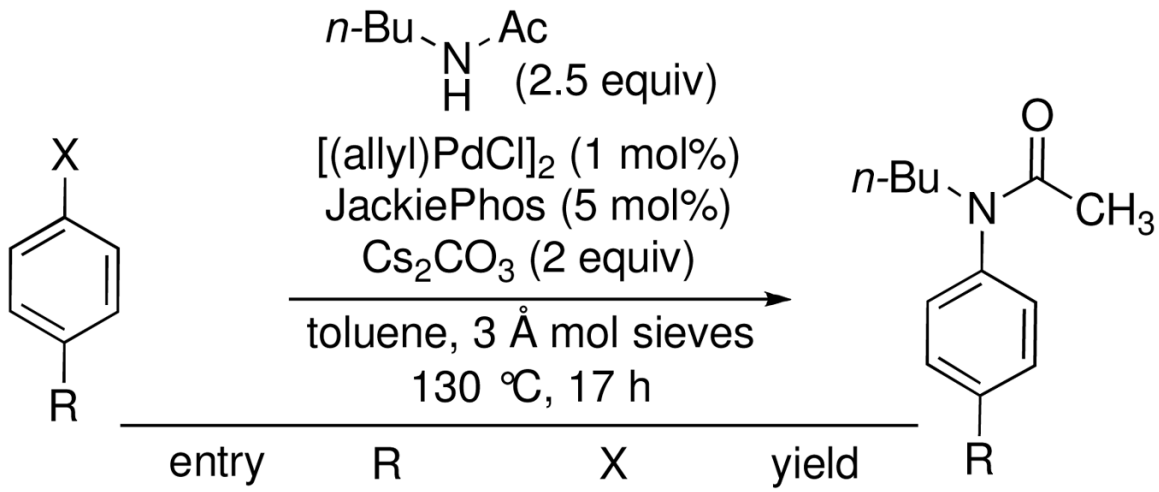

entry	R	X	yield
1	CH_3	OTf	78%
2	*n*-Bu	Cl	77%
3	CH_3	Br	67%
4	CH_3	I	3%

Table 7

Calculated Reaction Barriers for the Oxidative Addition of PhX with xantphos·Pd.

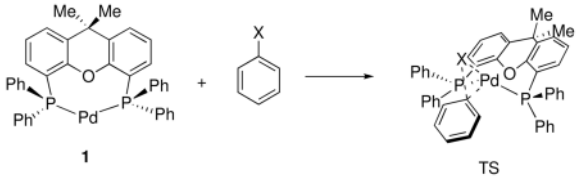

entry	TS	X	$\Delta G^{\ddagger}$ (kcal/mol)
1	**1-TS**	Br	26.8
2	**2-TS**	Cl	36.6

Table 8

d Angles and Bond Lengths.

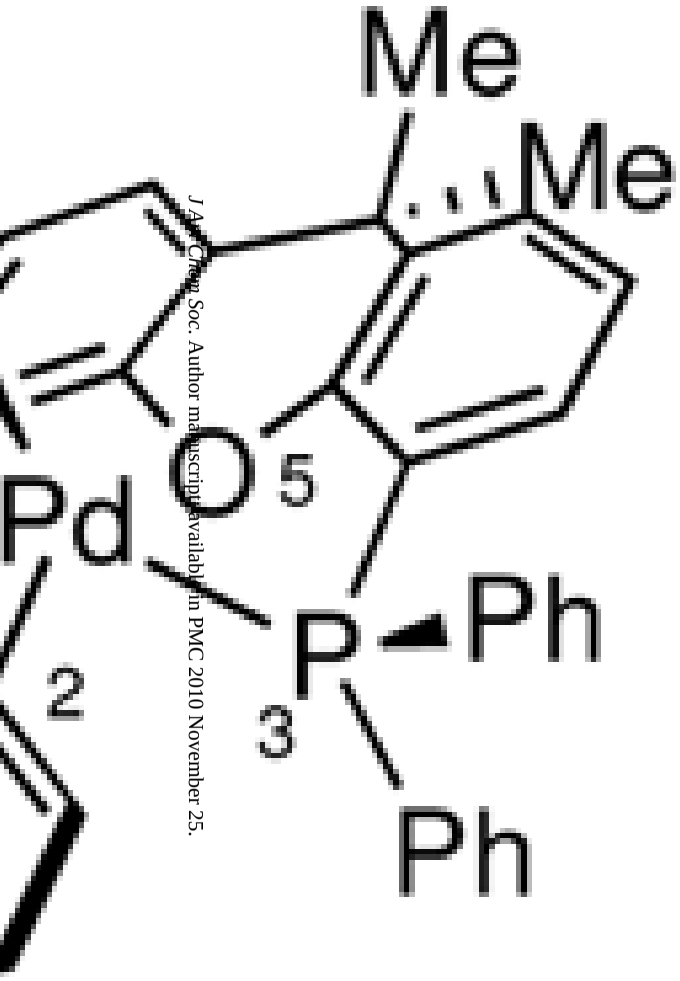

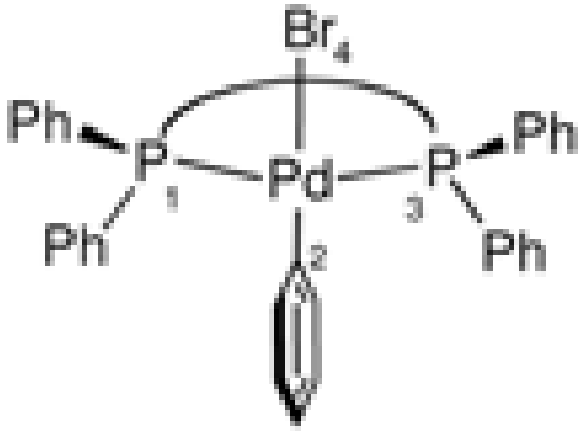

*xanthene backbone removed for clarity

2a

edral: ΔG_{rel} = +12.2 kcal/mol

	Bond Lengths (Å)	
	P1–Pd	2.55

2b

Trans: ΔG_{rel} = 0 kcal/mol

Bond Angles (deg)		Bond Lengths (Å)	
P1–Pd–P3	146.2	P1–Pd	2.38

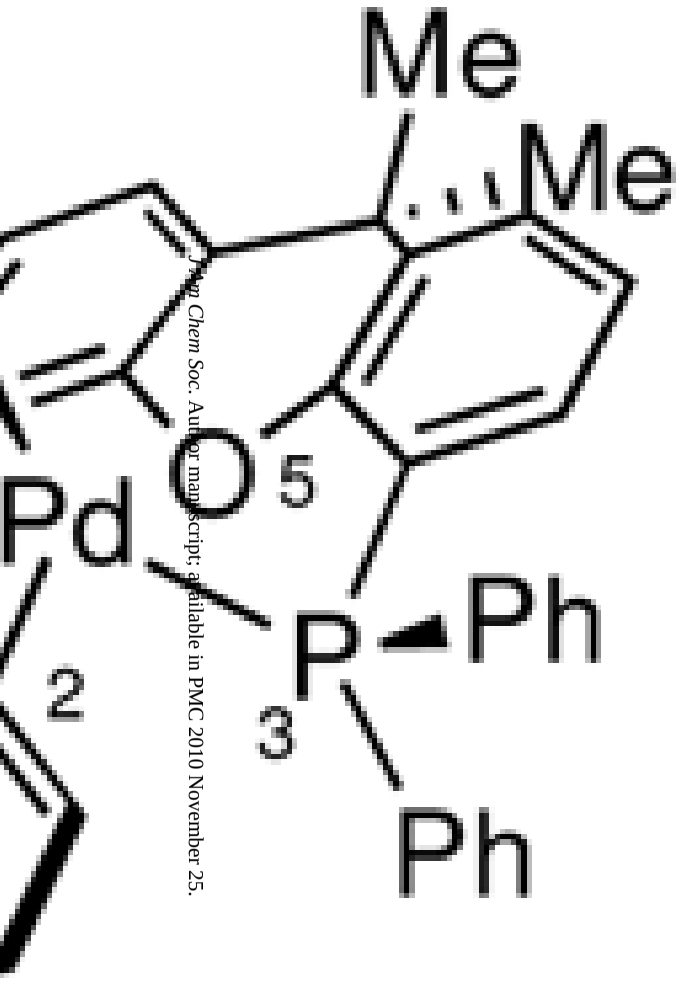

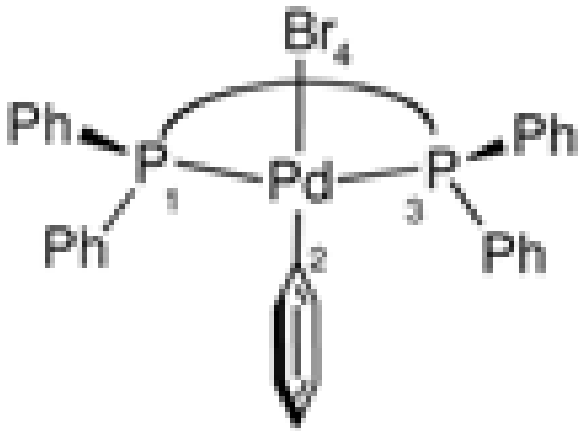

*xanthene backbone removed for clarity

2a

edral: ΔG_{rel} = +12.2 kcal/mol

	Bond Lengths (Å)		
	C2–Pd	1.98	

2b

Trans: ΔG_{rel} = 0 kcal/mol

Bond Angles (deg)		Bond Lengths (Å)	
P1–Pd–C2	92.5	C2–Pd	2.03

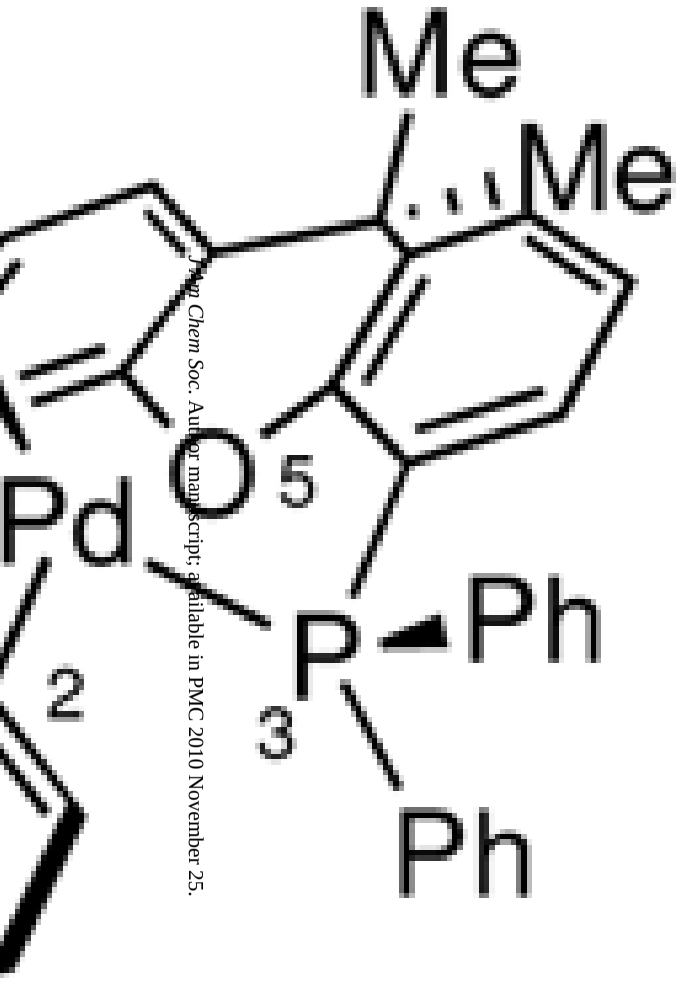

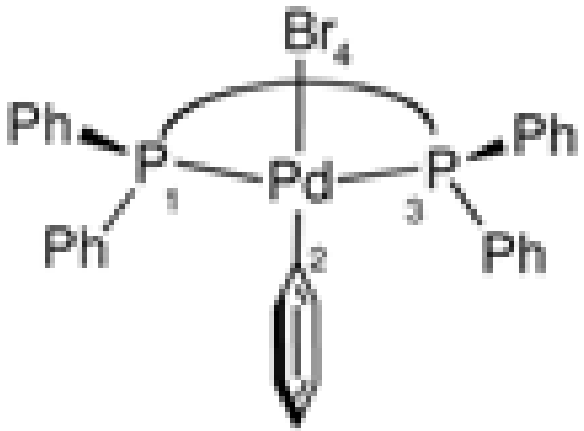

*xanthene backbone removed for clarity

2a

edral: ΔG_{rel} = +12.2 kcal/mol

	Bond Lengths (Å)	
	P3–Pd	2.55

2b

Trans: ΔG_{rel} = 0 kcal/mol

Bond Angles (deg)		Bond Lengths (Å)	
C2–Pd–P3	92.5	P3–Pd	2.38

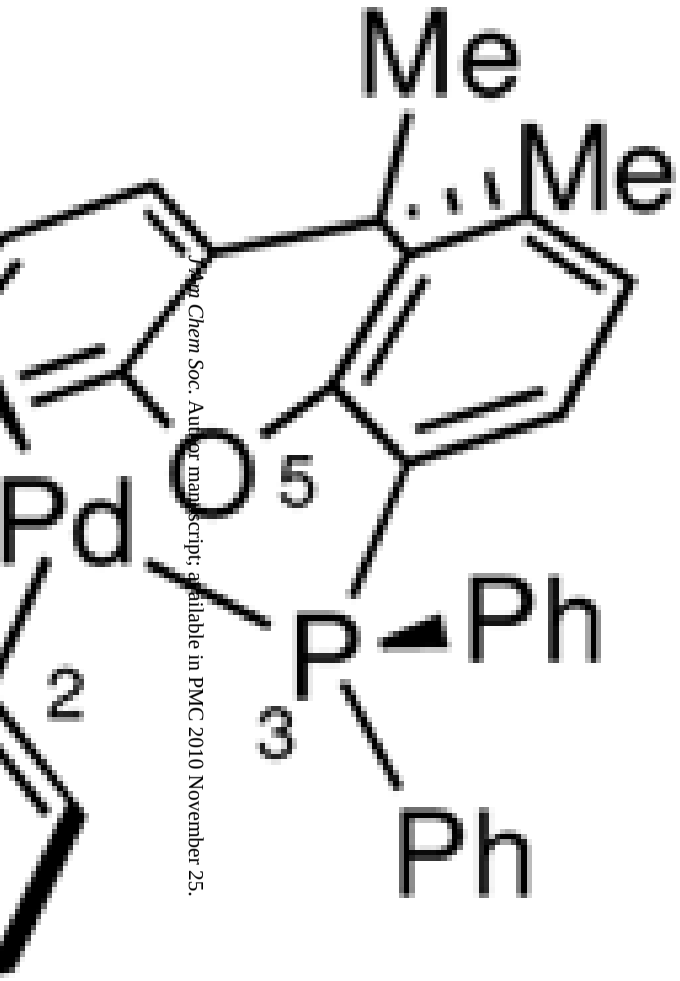

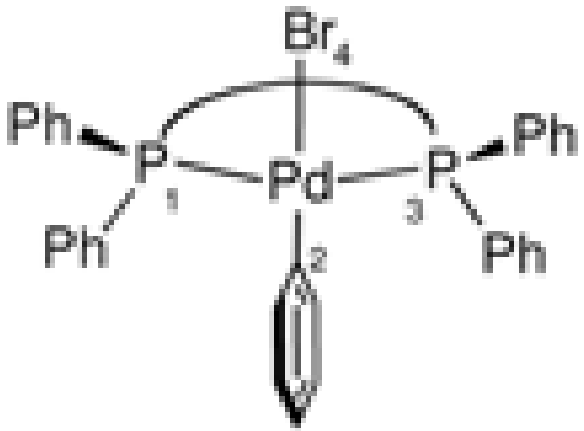

*xanthene backbone removed for clarity

2a

edral: ΔG_{rel} = +12.2 kcal/mol

	Bond Lengths (Å)	
	Br4–Pd	2.62

2b

Trans: ΔG_{rel} = 0 kcal/mol

Bond Angles (deg)		Bond Lengths (Å)	
P3–Pd–Br4	91.0	Br4–Pd	2.68

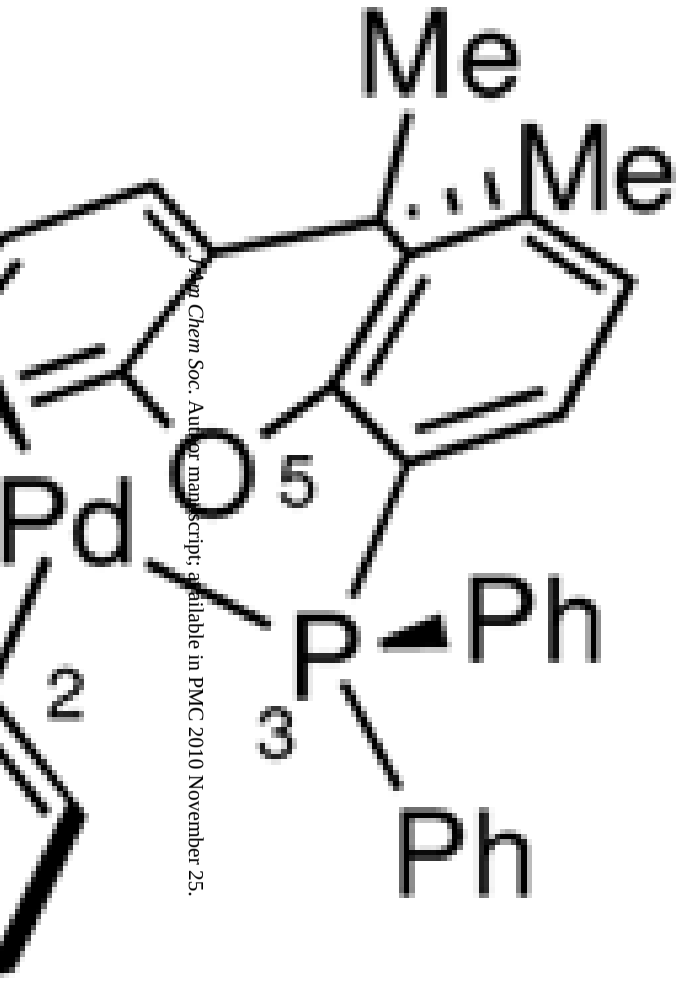

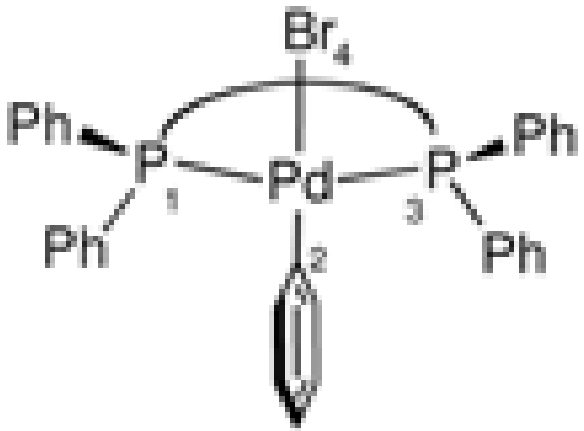

*xanthene backbone removed for clarity

2a

edral: ΔG_{rel} = +12.2 kcal/mol

	Bond Lengths (Å)	
	O5–Pd	3.17

2b

Trans: ΔG_{rel} = 0 kcal/mol

Bond Angles (deg)		Bond Lengths (Å)
Br4–Pd–P1	91.0	

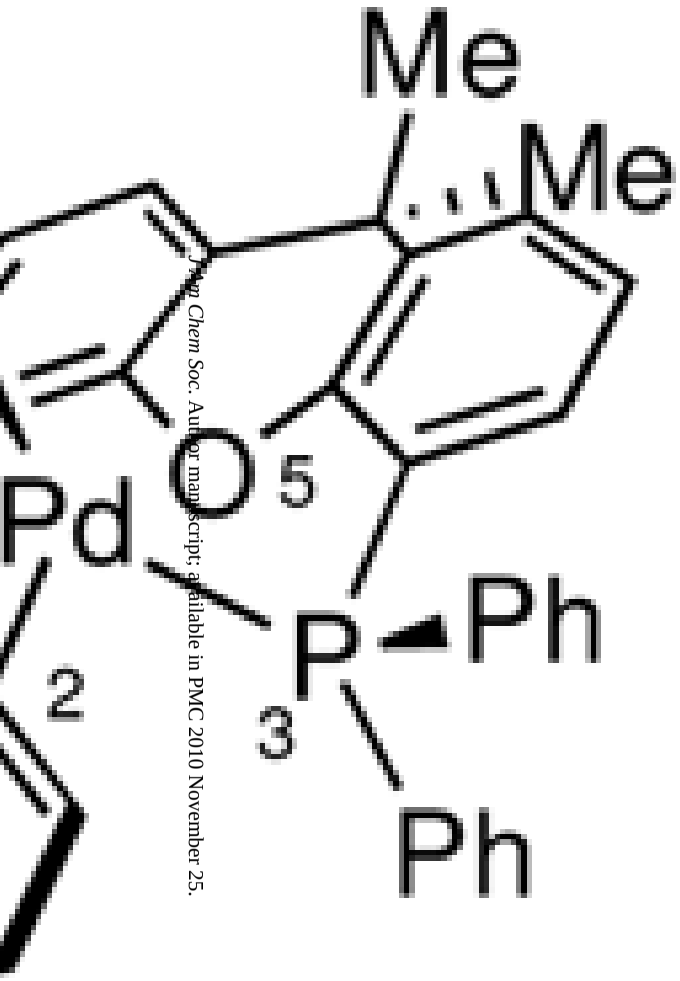

2a

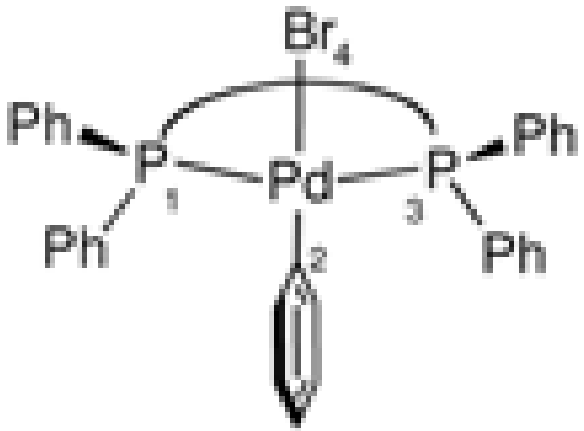

2b

*xanthene backbone removed for clarity

Bond Lengths (Å)

edral: ΔG_{rel} = +12.2 kcal/mol

Bond Angles (deg)		Bond Lengths (Å)
C2–Pd–Br4	167.7	

Trans: ΔG_{rel} = 0 kcal/mol

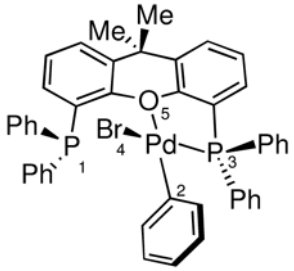

2c

O-bound: ΔG_{rel} = +4.0 kcal/mol

Bond Angles (deg)		Bond Lengths (Å)	
P3–Pd–C2	94.8	P1–Pd	3.27
C2–Pd–Br	92.4	C2–Pd	1.99
Br–Pd–O5	97.6	P3–Pd	2.33
O5–Pd–P3	76.0	Br4–Pd	2.57
Br4–Pd–P3	161.2	O5–Pd	2.49
O5–Pd–C2	169.9		

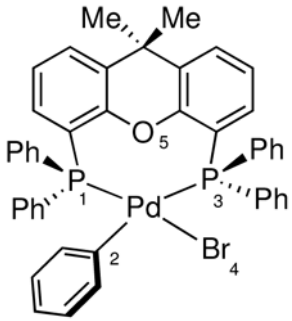

2d

cis: ΔG_{rel} = +2.1 kcal/mol

Bond Angles (deg)		Bond Lengths (Å)	
P1–Pd–P3	104.9	P1–Pd	2.42
P1–Pd–C2	89.3	C2–Pd	2.02
C2–Pd–Br4	83.6	P3–Pd	2.64
P3–Pd–Br4	86.5	Br4–Pd	2.60
Br4–Pd–P1	155.8	O5–Pd	3.59
C2–Pd–P3	163.7		

Table 9

Calculated Reaction Barriers for the Oxidative Addition of PhCl with L_1Pd.

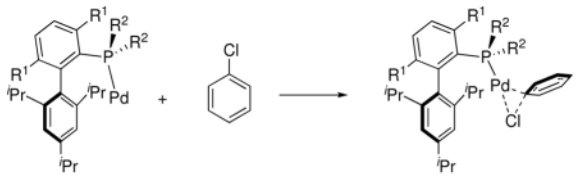

GS TS

entry	GS	TS	R^1	R^2	$\Delta G^{\ddagger}$ (kcal/mol)
1	**3**	**3-TS**	2,5-OMe	3,5-CF_3Ph	20.1
2	**4**	**4-TS**	2,5-OMe	Cy	10.8
3	**5**	**5-TS**	2,5-OMe	*t*-Bu	20.1
4	**6**	**6-TS**	2,5-OMe	Ph	16.5
5	**7**	**7-TS**	2-Me	3,5-CF_3Ph	20.4

Table 10

Calculated Binding Energies of *N*-Methyl Acetamide to L_1·Pd(Ph)(Cl).[a]

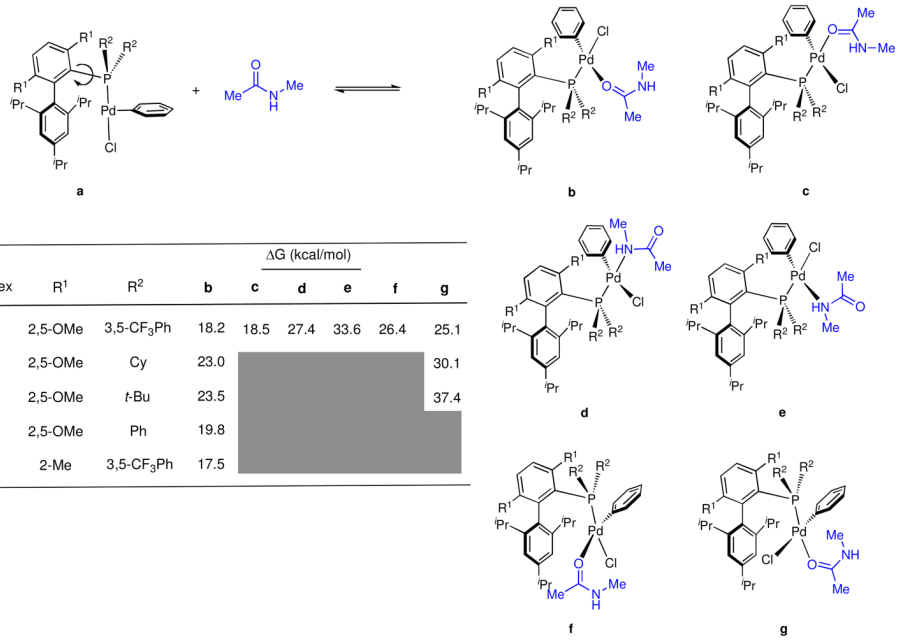

			ΔG (kcal/mol)					
complex	R^1	R^2	**b**	**c**	**d**	**e**	**f**	**g**
9	2,5-OMe	3,5-CF_3Ph	18.2	18.5	27.4	33.6	26.4	25.1
10	2,5-OMe	Cy	23.0					30.1
11	2,5-OMe	*t*-Bu	23.5					37.4
12	2,5-OMe	Ph	19.8					
13	2-Me	3,5-CF_3Ph	17.5					

[a] ΔG_{rel} is in reference to isomer **a** of each complex and *N*-methyl acetamide.

Table 11

Barriers to Rotation About the C2–P3 Bond for each L_1Pd(Ph)(amidate) Complex.

entry	ligand	maxima (deg)	ΔG (kcal/mol)[a]
1	JackiePhos	80	19.2
2	BrettPhos	90	20.5
3	*t*-Bu_2BrettPhos	80	27.7
4	Ph_2BrettPhos	80	19.1
5	**L10**	80	23.3

[a]The electronic energies of structures corresponding to the indicated dihedral angle were recalculated at 6-311+g(2d,p) with CPCM solvation correction and zero-point energy correction.

Table 12

Dissociative Mechanism for xantphos·Pd(Ph)(X).

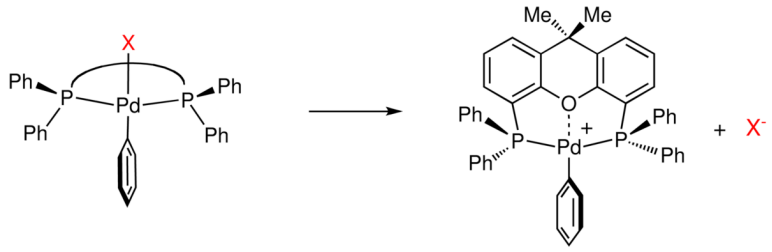

GS **14**

X	GS	ΔG (kcal/mol)
Br	**2b**	17.5
OTf	**15**	0.8

Table 13

Dissociative Mechanism for JackiePhos·Pd(Ph)(X).

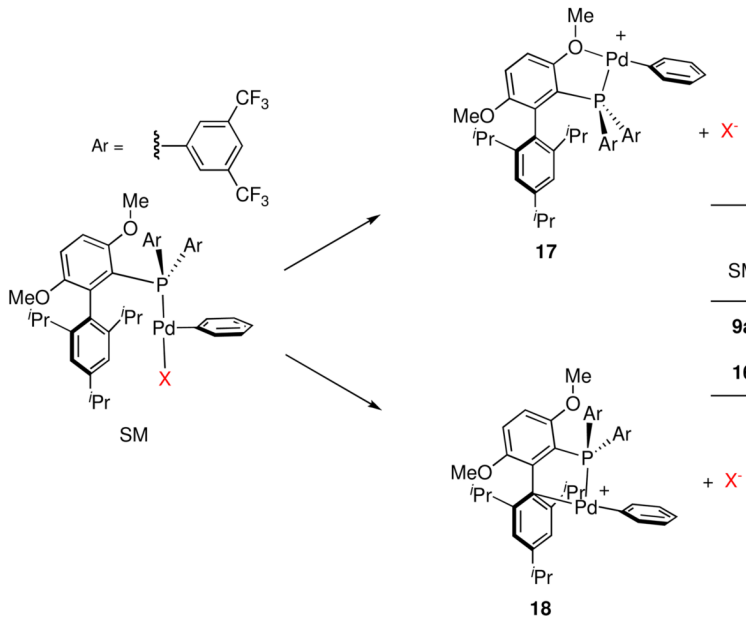

		ΔG (kcal/mol)	
SM	X	SM→**17**	SM→**18**
9a	Cl	62.0	42.9
16	OTf	54.0	34.9

κ^2-Binding of the Amide to Pd

Table 14

Calculated Barriers for Reductive Elimination of L_1·Pd(Ph)(amidate).

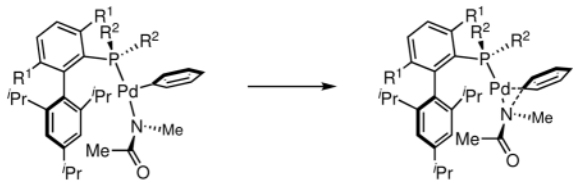

GS TS

entry	GS	TS	R^1	R^2	$\Delta G^{\ddagger}$ (kcal/mol)
1	**21**	**9-TS**	2,5-OMe	3,5-CF_3Ph	17.7
2	**24**	**10-TS**	2,5-OMe	Cy	19.7
3	**25**	**11-TS**	2,5-OMe	*t*-Bu	16.6
4	**26**	**12-TS**	2,5-OMe	Ph	20.0
5	**27**	**13-TS**	2-Me	3,5-CF_3Ph	16.6

Table 15

Calculated Energy Required for Catalytic Cycle Through Amide Binding (Not Including Deprotonation or Reductive Elimination).

ligand	ΔG (kcal/mol)
xantphos	32.0[a]
JackiePhos	18.2[b]
BrettPhos	23.0[b]
t-Bu_2BrettPhos	23.5[b]
Ph_2BrettPhos	19.8[b]
L10	17.5[b]

[a] Difference in energy from lowest energy state (**1**) and amide binding (**8**) in Figure 4.

[b] Difference in energy from lowest energy state (**C**) and amide binding (**E**) in Figure 5.